Probing the neutrino mass with calorimetric electron capture spectroscopy

Andrea Giachero

University & INFN of Milano-Bicocca

Neutrino: known facts

HOLMES

- The discovery of neutrino flavor oscillations has provided convincing evidence for non-zero neutrino masses and leptonic mixing
  - 3 active neutrino flavors: ν_e, ν_μ, ν_τ;
  - Neutrino flavor states are mixture of mass states: ν_1, ν_2, ν_3

$$|\nu_\alpha\rangle = \sum_j U_{\alpha j} |\nu_j\rangle \text{ with } \begin{cases} |\nu_\alpha\rangle & \text{: Flavor weak eigenstate;} \\ U_{\alpha j} & \text{: Neutrino mixing matrix;} \\ |\nu_j\rangle & \text{: Mass eigenstate.} \end{cases}$$

- In a three neutrino model, these oscillations are described by:
  - three angles: $\theta_{12}, \theta_{23}, \theta_{13}$;
  - two mass splittings: $\Delta m^2_{12}, |\Delta m^2_{23}|$;
    Δm^2_{12}: solar+reactor
    $|\Delta m^2_{23}|$: atmospheric+accelerator
  - one CP violating phase: δ_{CP};
  - two Majorana phases: α_1, α_1.
    physically meaningful only if neutrinos are Majorana particles

- Global analysis with different sources and different experimental techiniques:

$$U = \underbrace{\begin{bmatrix} 1 & 0 & 0 \\ 0 & c_{23} & s_{23} \\ 0 & -s_{23} & c_{23} \end{bmatrix}}_{\text{Atmospheric and accelerator experiments}} \cdot \underbrace{\begin{bmatrix} c_{13} & 0 & s_{13}e^{-i\delta_{CP}} \\ 0 & 1 & 0 \\ -s_{13}e^{-i\delta_{CP}} & 0 & c_{13} \end{bmatrix}}_{\text{Reactor and accelerator experiments}} \cdot \underbrace{\begin{bmatrix} c_{12} & s_{12} & 0 \\ -s_{12} & c_{12} & 0 \\ 0 & 0 & 1 \end{bmatrix}}_{\text{Solar and accelator experiments}} \cdot \underbrace{\begin{bmatrix} e^{-i\alpha_1} & 0 & 0 \\ 0 & e^{-i\alpha_2} & 0 \\ 0 & 0 & 1 \end{bmatrix}}_{0\nu\beta\beta \text{ experiments}}$$

$$\Delta m^2_{ij} = m^2_i - m^2_j \ , \ s_{ij} = \sin\theta_{ij} \ , \ c_{ij} = \cos\theta_{ij}$$

Neutrino: global analysis

parameter	Best-fit ± 1σ	2σ range	3σ range
Δm^2_{21} [10^{-5}eV^2]	$7.55^{+0.20}_{-0.16}$	7.20–7.94	7.05–8.14
$\lvert\Delta m^2_{31}\rvert$ [10^{-3}eV^2] (NO)	2.50 ± 0.03	2.44–2.57	2.41–2.60
$\lvert\Delta m^2_{31}\rvert$ [10^{-3}eV^2] (IO)	$2.42^{+0.03}_{-0.04}$	2.34–2.47	2.31–2.51
$\sin^2\theta_{12}/10^{-1}$	$3.20^{+0.20}_{-0.16}$	2.89–3.59	2.73–3.79
$\sin^2\theta_{23}/10^{-1}$ (NO)	$5.47^{+0.20}_{-0.30}$	4.67–5.83	4.45–5.99
$\sin^2\theta_{23}/10^{-1}$ (IO)	$5.51^{+0.18}_{-0.30}$	4.91–5.84	4.53–5.98
$\sin^2\theta_{13}/10^{-2}$ (NO)	$2.160^{+0.083}_{-0.069}$	2.03–2.34	1.96–2.41
$\sin^2\theta_{13}/10^{-2}$ (IO)	$2.220^{+0.074}_{-0.076}$	2.07–2.36	1.99–2.44
δ_{CP}/π (NO)	$1.32^{+0.21}_{-0.15}$	1.01–1.75	0.87–1.94
δ_{CP}/π (IO)	$1.56^{+0.13}_{-0.15}$	1.27–1.82	1.12–1.94

The results for inverted mass ordering were calculated with respect to this mass ordering.

- $\Delta m^2_{21} = \Delta m^2_{\odot} \simeq 75\,\mu\,\mathrm{eV}^2$
- $|\Delta m^2_{31}| = |\Delta m^2_{\mathrm{atm}}| \simeq (2.4 - 2.5)\,\mathrm{m\,eV}^2$
- $\theta_{12} = \theta_{\odot} \simeq 35^\circ$
- $\theta_{13} = \simeq 8.5^\circ$
- $\theta_{23} = \theta_{\mathrm{atm}} \simeq 45^\circ$

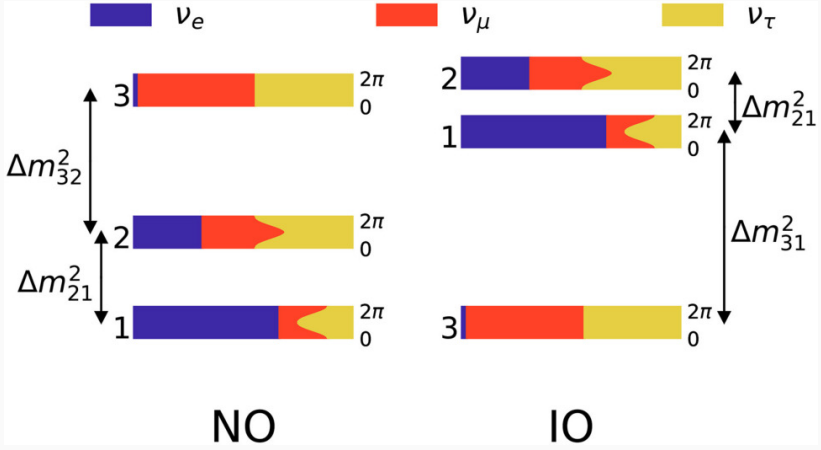

(more details on Front. Astron. Space Sci. 5 (2018) 36 and Phys. Lett. B 782 (2018) 633–640)

HOLMES

Future oscillation experiments can:

- perform a precise measurement of the mixing angles θ_{ij}

  $\Rightarrow$ determination of the octant in which θ_{23} lies;
  (low-octant: $\theta_{23} < 45°$, high-octant: $\theta_{23} > 45°$)

- determinate of the neutrino mass ordering: the sign of $\Delta m^2_{32,31} = m^2_3 - m^2_{2,1}$
  - Normal hierarchical (NH): $m_1 \ll (<) m_2 \ll m_3 \Rightarrow \Delta m^2_{32,31} > 0$
  - Inverted hierarchical (IH): $m_3 \ll m_1 \lesssim m_2 \Rightarrow \Delta m^2_{32,31} < 0$

  $\Rightarrow$ currently a 3σ hint for Normal Hierarchy (NH) (arXiv:1811.05487 [hep-ph]);

- search for CPV in neutrino oscillations

  $\Rightarrow$ current preferred values of δ_{CP} in the range $[\pi, 2\pi]$ (Phys. Lett. B 782 (2018) 633–640)

Future oscillation experiments can not:

- provide information about neutrino nature: Dirac ($\nu \neq \overline{\nu}$) or Majorana ($\nu = \overline{\nu}$)

  $\Rightarrow$ but generation of $0\nu\beta\beta$ experiments could

- provide information about Majorana phases

  $\Rightarrow$ oscillation combined with next generation of $0\nu\beta\beta$ experiments could

- provide information about neutrino absolute mass

  $\Rightarrow$ cosmology, $0\nu\beta\beta$ and direct neutrino mass experiments could

HOLMES

Constraint from cosmology:

- Cosmic microwave background (CMB);
- Galaxy clustering;
- Lyman-alpha forest;
- Weak lensing.

Observable	$m_\Sigma = \sum_k m_i$
Best limit	$m_\Sigma \leq 0.140$ eV @ 95% by combining different data

Constraint from the Neutrinoless Double Beta-Decay ($0\nu\beta\beta$):

- Forbidden by Standard Model ($\Delta L = 2$);
- Allowed only for Majorana neutrino;
- Never observed.
- $\left[\tau_{1/2}^{0\nu}\right]^{-1} = G^{0\nu}\left|M^{0\nu}\right|^2\left|\langle m_{\beta\beta}\rangle\right|^2$
- $m_{\beta\beta}$: Effective Majorana Mass

Decay	$(A,Z) \rightarrow (A,Z+2) + 2e^-$
Observable	$m_{\beta\beta} = \lvert \sum_k m_i U_{ek}^2 \rvert$
Best limit	^{76}Ge: $m_{\beta\beta} \leq (140 \div 300)$ meV ^{100}Mo: $m_{\beta\beta} \leq (330 \div 620)$ meV ^{130}Te: $m_{\beta\beta} \leq (110 \div 520)$ meV ^{136}Xe: $m_{\beta\beta} \leq (61 \div 165)$ meV

Constraint from the Direct Neutrino Mass Determination:

- Kinematical analysis of the end point region of the β decay spectra;
- The neutrino is not directly observed but the energy of the decay products is precisely measured;

Decay	$(A,Z) \rightarrow (A,Z+1) + e^- + \overline{\nu}_e$ (βD) $(A,Z) + e^- \rightarrow (A,Z-1) + \nu_e$ (EC)
Observable	$m_\beta = \sqrt{\sum_k m_i^2 \lvert U_{ek}\rvert^2}$
Best limit	$m_\beta \leq 2.2$ eV

Neutrino mass: available experimental tools (cont.)

HOLMES

Tool	Cosmology	Double Beta Decay	Beta Decay End Point
Observable	$m_\Sigma = \sum_k m_i$	$m_{\beta\beta} = \lvert \sum_k m_i U_{ek}^2 \rvert$	$m_\beta = \sqrt{\sum_k m_i^2 \lvert U_{ek} \rvert^2}$
Present Sensitivity	$\simeq 0.1$ eV	$\simeq 0.1$ eV	2 eV
Future Sensitivity	0.01 eV	0.01 eV	0.2 eV
Model Dependency	yes ☹	yes ☹	no ☺
Systematics	large ☹	small ☺	large ☹

Cosmology

- The parameter m_Σ suffers of cosmological model dependency ☹

Neutrinoless Double Beta

- The calculations of nuclear matrix elements of $0\nu\beta\beta$-decay is a challenge for nuclear physics (several different approach, model dependency) ☹

Beta Decay end-point measurement

- The measurement of the end point of nuclear beta or electron capture (EC) decays spectra is the only model-independent ☺

β-decay and neutrino mass

- Study of the *visible* energy of the decay
  - $\lambda = 2\pi \left|M\right|^2 \rho_f$ (Fermi Golden Rule)
  - $\frac{d\lambda}{dE} = (Q-E)\sqrt{(Q-E)^2 - m_\beta^2}$

    $(E \equiv E_e - m_e, \quad Q \equiv \max(E) \text{ for } m_\nu = 0)$

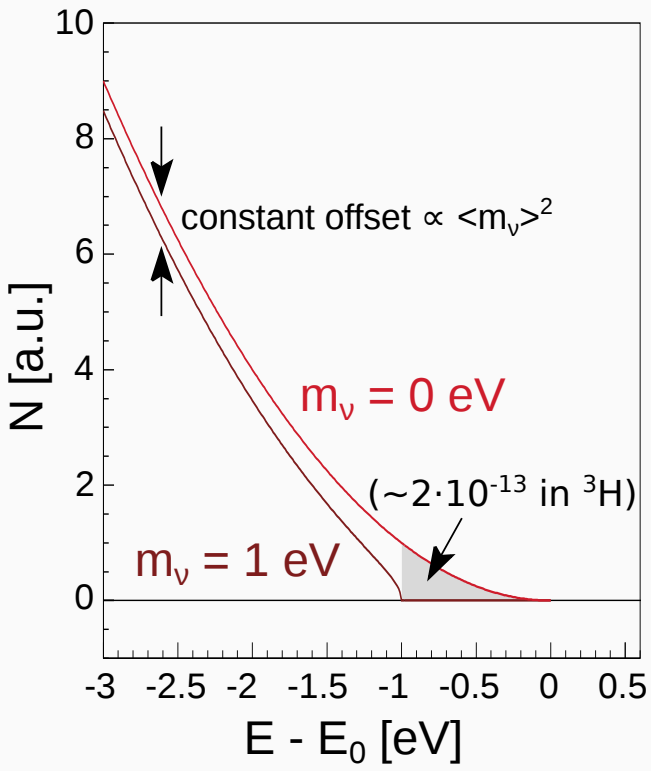

- High statistics at the beta spectrum end-point
  - Low end-point energy Q: $F(\delta E) \simeq (\delta E/Q)^3$;
  - High source activity and high efficiency

- High energy resolution ΔE:
  - *experimentally*, it is easier to get better ΔE at lower energies

Requirements:

- low Q
- short half-lives

β-decay: candidate isotopes

- ^{3}H : $^{3}\mathrm{H} \rightarrow {}^{3}\mathrm{He} + e^- + \bar{\nu}_e \quad (\beta^-) \quad \Rightarrow \quad m_\nu < 2.2\,\mathrm{eV}$ @ 95% C.L.
  - $Q = 18.6\,\mathrm{keV}, \quad t_{1/2} = 12.3$ years
  - super-allowed transition (no lepton carries away angular momentum)
  - rather simple electronic structure also for molecular T_2

    Mainz, Troitsk, KATRIN, Project8, PTOLEMY

- ^{187}Re : $^{187}\mathrm{Re} \rightarrow {}^{187}\mathrm{Os} + e^- + \bar{\nu}_e \quad (\beta^-) \quad \Rightarrow \quad m_\nu < 15\,\mathrm{eV}$ @ 90% C.L.
  - $Q = 2.47\,\mathrm{keV}, \quad t_{1/2} = 4.3 \cdot 10^{10}$ years

    MANU, MIBETA, MARE

- ^{163}Ho : $^{163}\mathrm{Ho} \rightarrow {}^{163}\mathrm{Dy} + e^- + \bar{\nu}_e \quad (\mathrm{EC})$
  - $Q = 2.833\,\mathrm{keV}, \quad t_{1/2} = 4570$ years
  - de-excitation spectrum of intermediate $^{163}\mathrm{Dy}^*$ ($\rightarrow$ series of lines)

    ECHo, HOLMES, NuMECS;

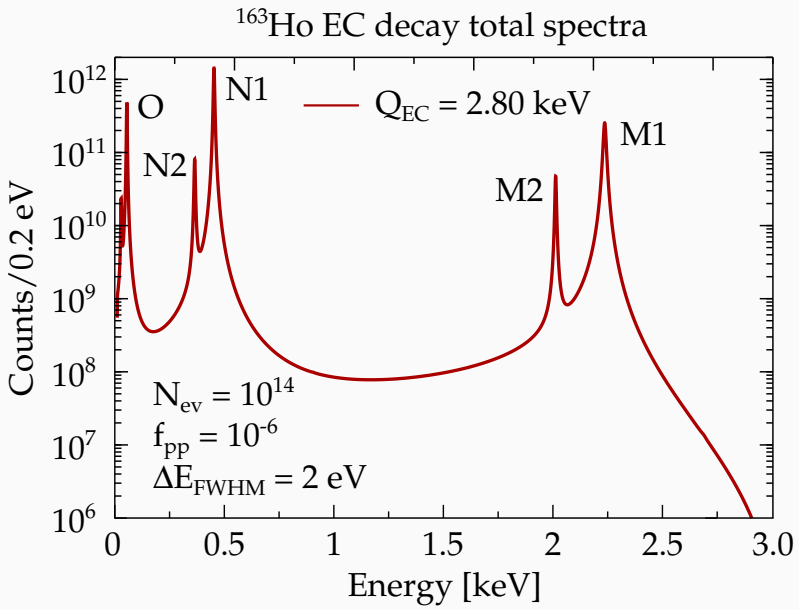

suitable for low temperature micro-calorimeter

concluded running R&D/Construction

HOLMES

Spectrometers: source $\neq$ detector

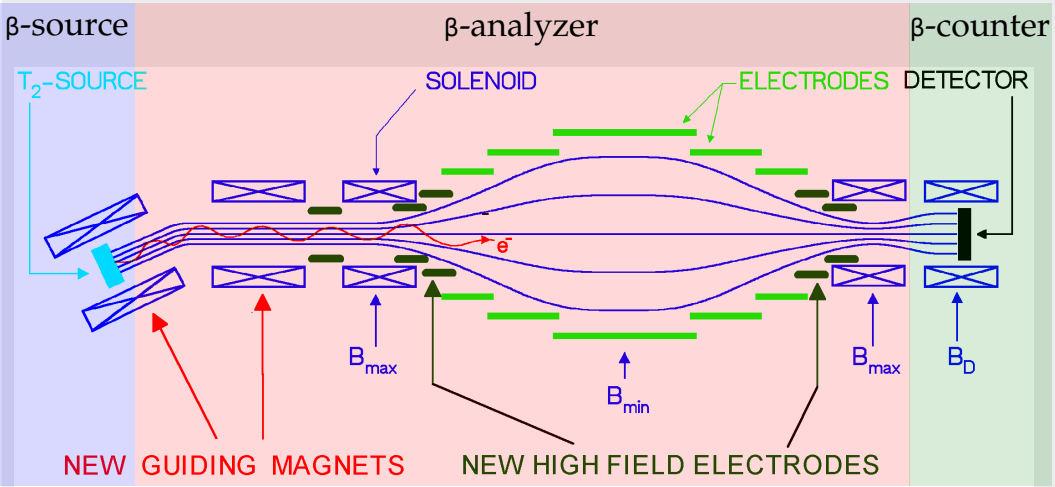

(Mainz spectrometer, sketch-up from Eur. Phys. J. C 73 (2013) 2323)

- Tritium β decay: $^3\mathrm{H} \rightarrow ^3\mathrm{He}^+ + \mathrm{e}^- + \overline{\nu}_e$
- Magnetic spectrometers and MAC-E filter;
- The β-electrons with enough energy to pass the MAC-E filter are detected;

Calorimeters: source $\subseteq$ detector

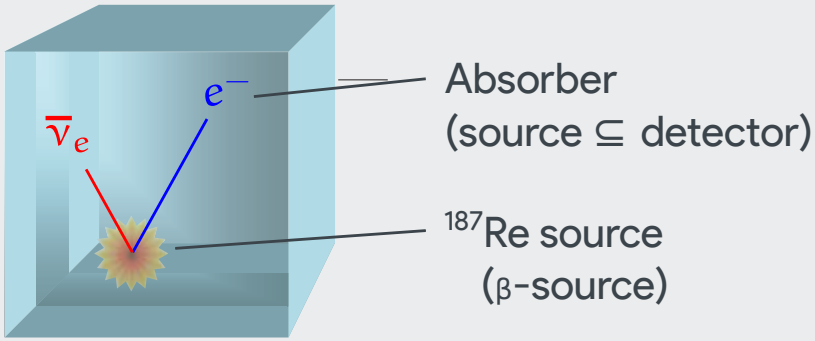

$$^{187}\mathrm{Re} \rightarrow {}^{187}\mathrm{Os} + \mathrm{e}^- + \overline{\nu}_e$$

- The β source is embedded in the detector (absorber);
- Ideally measurement of all the energy E released in the decay except for the ν_e energy;

Experimental approaches (cont.)

HOLMES

General experimental requirements:

- High statistics at the beta spectrum end-point:
  - Low end-point energy Q: $F(\delta E) \propto (\delta E/Q)^3$
    $\Rightarrow$ where δE is the energy range considered near the end point;
  - High source activity and high efficiency;
- High energy resolution ΔE (same order of magnitude of m_ν sensitivity);
- High signal-to-noise ratio (SNR);
- Small systematic effects.

Spectrometers: source $\neq$ detector:

☺ high statistics: $\tau_{1/2}(^3\mathrm{H}) = 12.3$ y;

☺ high energy resolution: $\Delta E \simeq 1$ eV;

☹ systematics due to source effect;

☹ systematics due to decay to excitated states;

☹ background.

Calorimeters: source $\subseteq$ detector:

☺ no backscattering;

☺ no energy losses in the source;

☺ no solid state excitation;

☺ no atomic/molecular final state effect;

☹ limited statistics: $\tau_{1/2}(^{187}\mathrm{Re}) \simeq 4 \cdot 10^{10}$ y;

☹ systematics due to pile-up;

☹ background.

Spectrometers: present results

Mainz Experiment: solid ^{3}H source (1997-2001)

$$m_\nu^2 = -0.6 \pm 2.2_{(stat)} \pm 2.1_{(sys)}\, eV^2$$

$$\Downarrow$$

$$m_\nu < 2.3\, eV\, (95\%\, C.L.)$$

Results after all critical systematics measured (atomic physics, surface and solid state physics, inelastic scattering, self-charging, neighbour excitation)

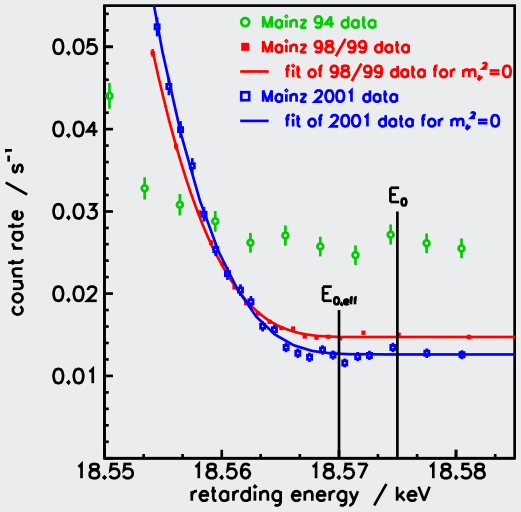

Troitsk Experiment: gaseous ^{3}H source (1997-2004)

$$m_\nu^2 = -0.67 \pm 1.89_{(stat)} \pm 1.68_{(sys)}\, eV^2$$

$$\Downarrow$$

$$m_\nu < 2.05\, eV\, (95\%\, C.L.)$$

Most significant systematics:

- Stability of source conditions;
- Energy loss inside tritium source;
- Background due to non-optimal vacuum;

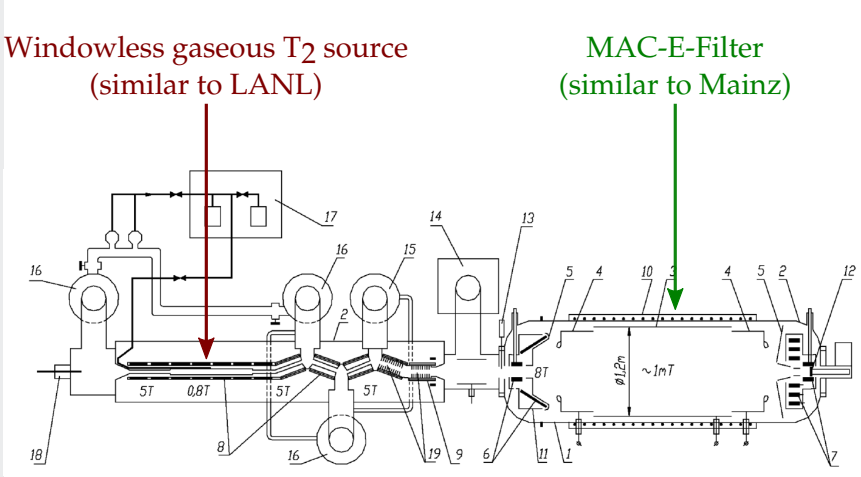

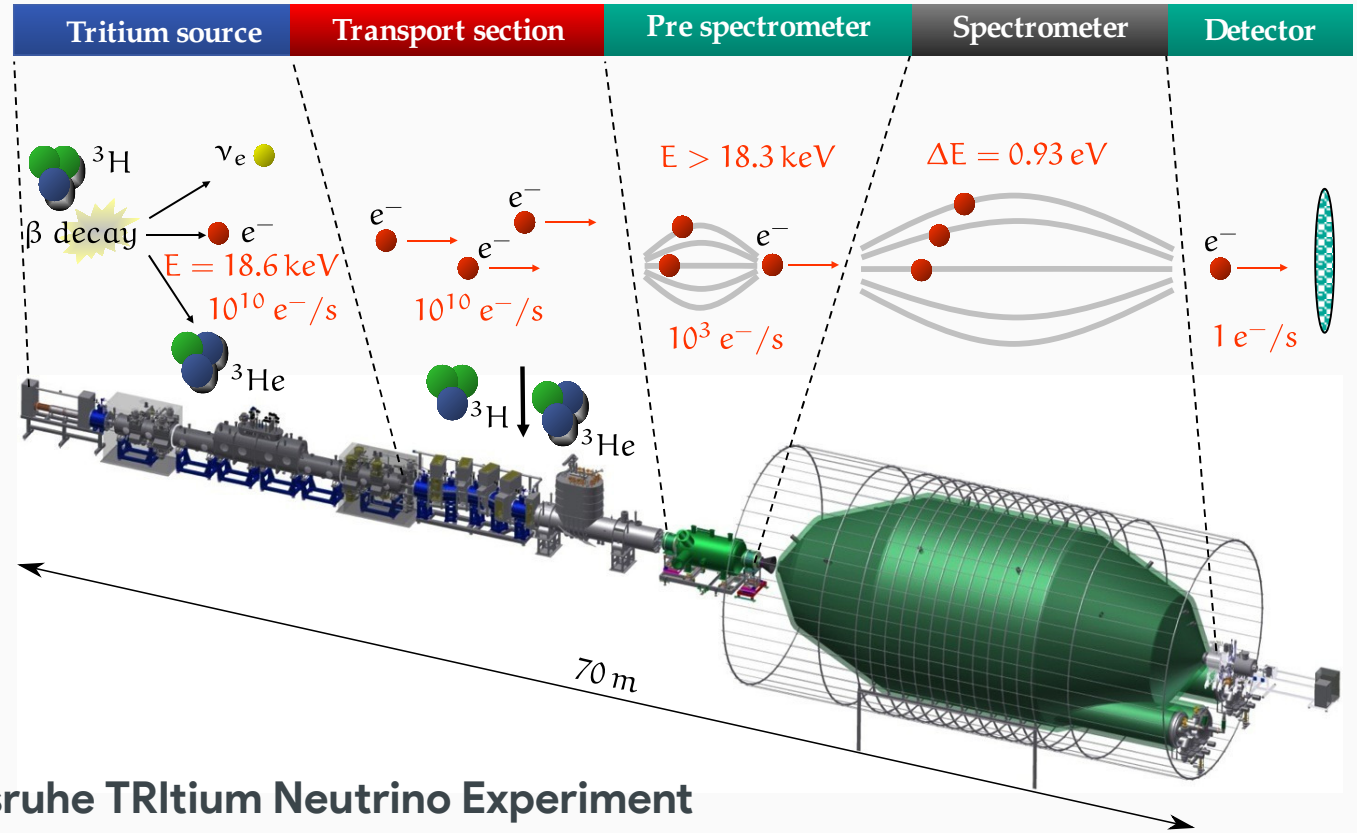

KATRIN
The KArlsruhe TRItium Neutrino Experiment

KATRIN Design Report FZKA scientific report 7090

- Larger electrostatic spectrometer ever built (stainless steel vessel, $\varnothing = 10$ m , $L = 22$ m);
- Intense Windowless Gaseous Tritium Source (WGTS): 10^{11} β decay electrons per second;
- Energy resolution: $\Delta E = 0.93$ eV;
- High luminosity: $L = 20$ cm^2 (Troitsk: $L = 0.6$ cm^2);
- Ultrahigh vacuum requirements: $p < 10^{-11}$ mbar (to reduce the background).
- Very first tritium from May 2018 $\Rightarrow$ data-taking in progress.

Expected statistical sensitivity: $m_\nu < 0.2$ eV @ 90% C.L.

The use of low temperature detectors (LTD)

HOLMES

- Low temperature detectors play key role in several frontier sectors of neutrino physics;
- Suggested as high resolution soft X-ray detectors in 1984 by D. McCammon and collaborators
  S.H. Moseley, J.C. Mather, D. McCammon, J. Appl. Phys. 56 (1984) 1257;
- First proposed for neutrino physics experiments in 1984 by E. Fiorini and T. Niinikoski
  E. Fiorini and T. Niinikoski, Nucl. Instrum. and Meth. 224 (1984) 83-88;

CMB

As bolometers

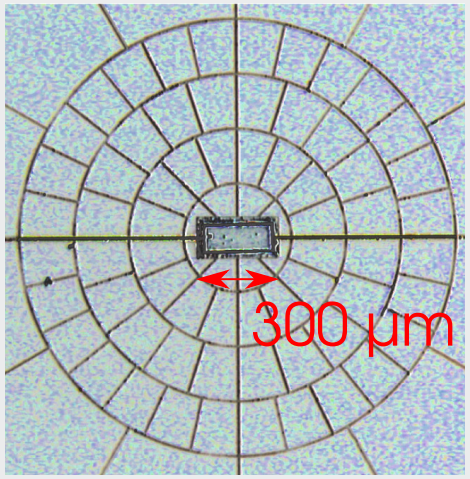

Planck

β-decay

As micro-calorimeters

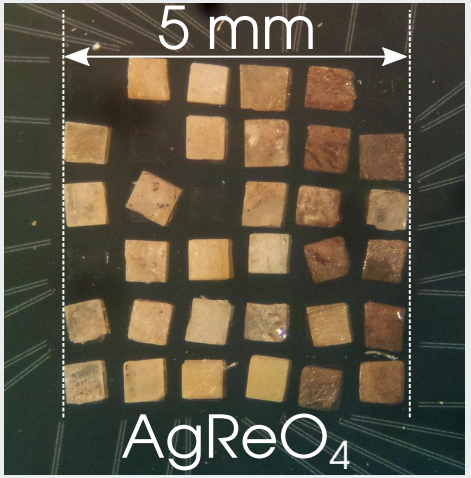

MARE

$0\nu\beta\beta$

As large-calorimeters

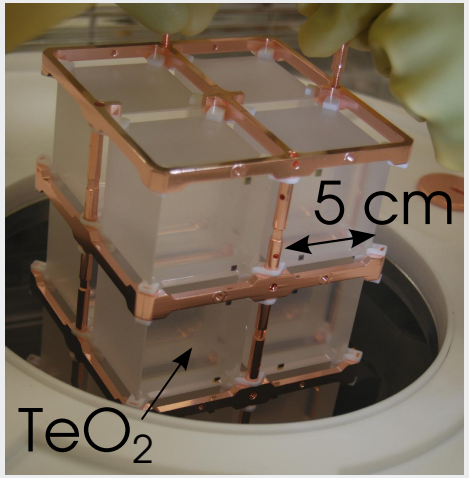

CUORE-0

Low Temperature Detectors as Calorimeters

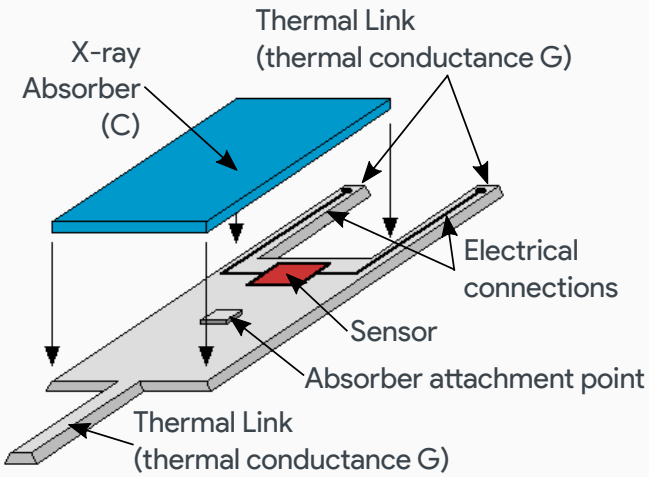

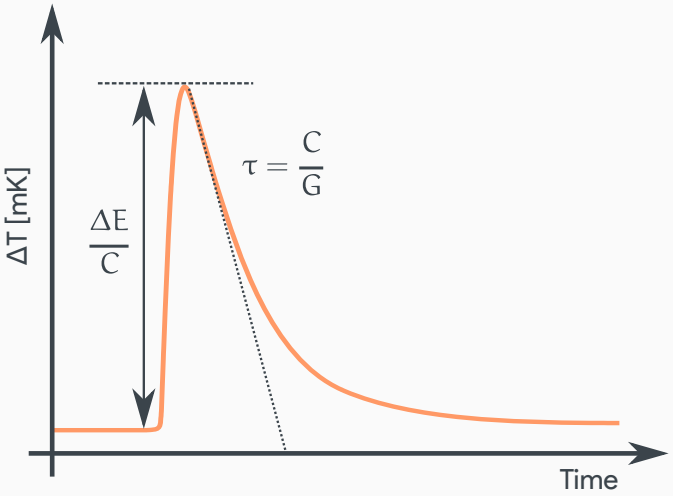

- A Low Temperature Calorimeter $\Rightarrow$ senses the heat generated by a particle absorbed and thermalized in a very low heat capacity element
- Complete energy thermalization: ionization, excitation $\Rightarrow$ heat $\Rightarrow$ calorimetry;
- $\Delta T = \Delta E/C$ where ΔE is the released energy and C the total thermal capacity;
  - Absorber with very low thermal capacity: $C \downarrow \quad \Rightarrow \quad \Delta T \uparrow$;
  - Debye low for superconductors below T_C and dielectric: $C \propto (T/\Theta_D)^3$;
  - A very low temperature is needed: $T \downarrow \Rightarrow C \downarrow \Rightarrow \Delta T \uparrow \Rightarrow (T = 10 \div 100\ \text{mK})$;
- Limit to energy resolution $\Rightarrow$ statistical fluctuation of internal energy $\Delta E_{rms} = \sqrt{k_B T^2 C}$;

LTD: several configurations and applications

HOLMES

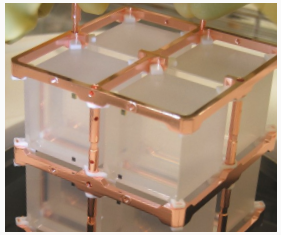

Type: macro
Absorber: TeO_2
Sensor: NTD Ge-thermistor
Application: $0\nu\beta\beta$
CUORICINO, CUORE-0
CUORE

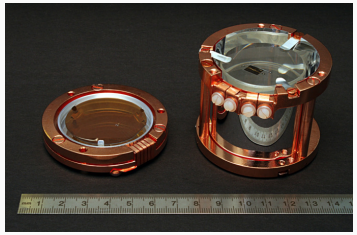

Type: macro
Absorber: $CaWO_4$
Sensor: TES
Application: Dark Matter
CRESST

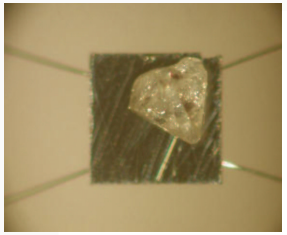

Type: micro
Absorber: $AgReO_4$
Sensor: Si-thermistor
Application: β-decay
MiBeta (concluded)

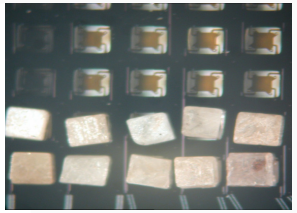

Type: micro
Absorber: $AgReO_4$
Sensor: Si-thermistor
Application: β-decay
Mare (concluded)

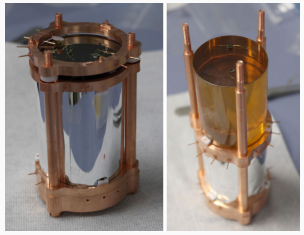

Type: macro
Absorber: ZnSe
Sensor: NTD Ge thermistor
Application: $0\nu\beta\beta$
LUCIFER/CUPID-0

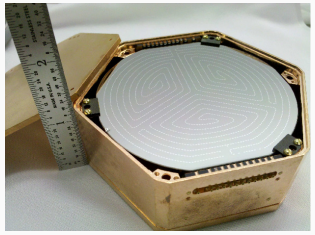

Type: macro
Absorber: Ge
Sensor: TES
Application: Dark Matter
CDMS/SuperCDMS

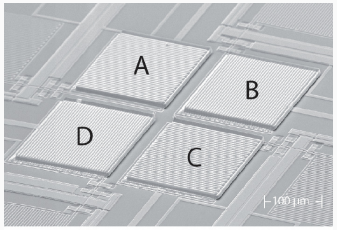

Type: micro
Absorber: Gold
Sensor: Au:Er alloy MMC
Application: β-decay
ECHo

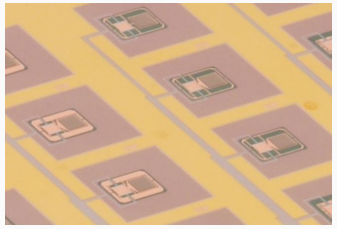

Type: micro
Absorber: Gold
Sensor: Mo/Cu TES
Application: β-decay
HOLMES

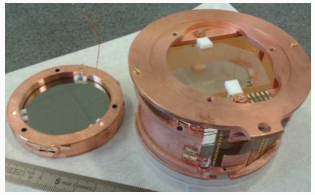

Type: macro
Absorber: $ZnMoO_4$
Sensor: NTD Ge thermistor
Application: $0\nu\beta\beta$
LUMINEU

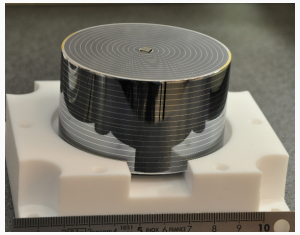

Type: macro
Absorber: Germanium
Sensor: InterDigit Ge-NTD
Application: Dark Matter
EDELWEISS-III

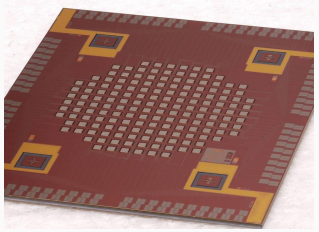

Type: micro
Absorber: Bismuth
Sensor: Mo/Cu TES
Application:
X-ray Spectroscopy

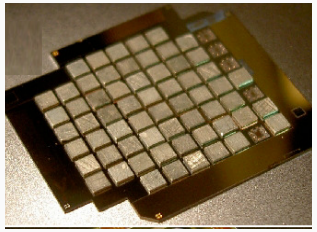

Type: micro
Absorber: Tin
Sensor: Mo/Cu TES
Application:
γ-ray Spectroscopy

Temperature Sensors

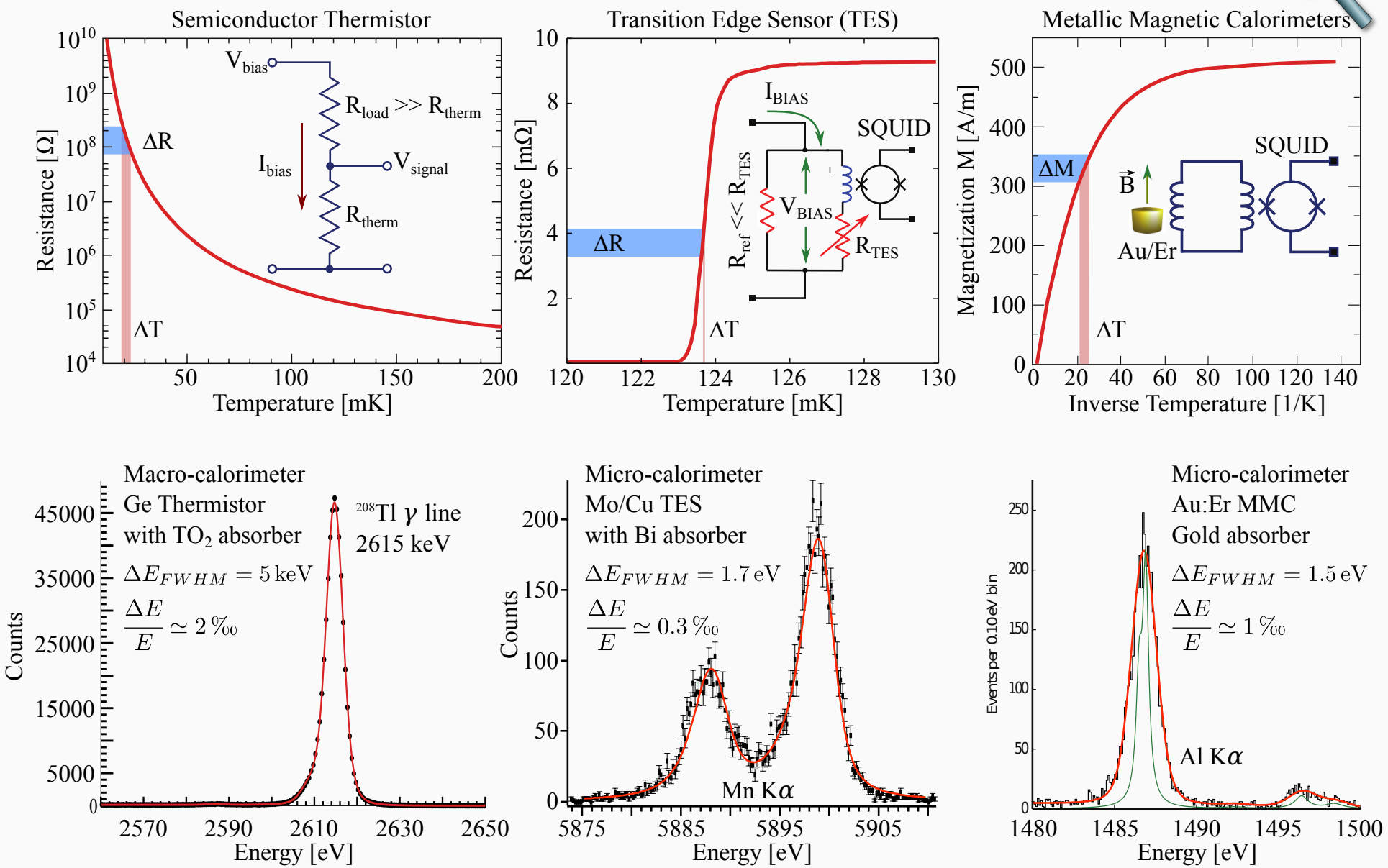

Plots from A. Giachero, J. Phys. Conf. Ser. 841 (2017) 012027

Microcalorimeters for β-decay

HOLMES

Isotope candidate: ^{187}Re β decay $\Rightarrow$ $^{187}Re \rightarrow {}^{187}Os + e^- + \overline{\nu}_e$

Rhenium is perfectly suited for fabricating thermal detectors.

- Dielectric or superconductor behaviour;
- Very low end point: $Q = 2.47$ keV;
- Half-life time: $\tau_{1/2} = 43.2$ Gy;
- High natural abundance: a.i. $= 63\%$;
- Rate of 1 mg metallic Rhenium: $\simeq 1.0$ decay/s.

Metallic Rhenium single crystals

- Absorber: Re superconductor with $T_C = 1.6$ K;
- Sensor: NTD thermistors;
- MANU experiment (Genova).

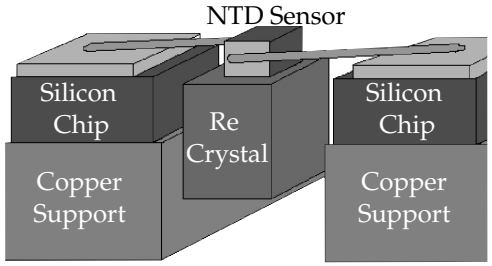

Dielectric Rhenium compound ($AgReO_4$) crystals

- Absorber: $AgReO_4$ crystals (Silver perrhenate);
- Sensor: Silicon implanted thermistors;
- MIBETA experiment (Milano, Como, Trento).

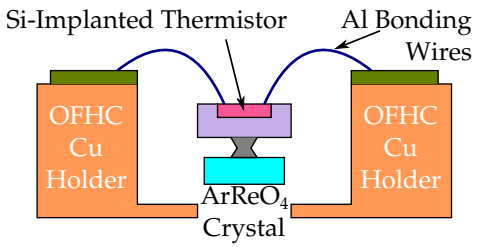

Microcalorimeters for β-decay: present results

HOLMES

MANU (1999)

- 1 crystal of metallic Re: 1.6 mg;
- ^{187}Re activity: $\simeq$ 1.6 Hz;
- Sensor: Ge NTD thermistor:
- Resolution: $\Delta E = 96$ eV FWHM;
- Live-time: 0.5 years;
- $6.0 \cdot 10^6$ ^{187}Re decays above 420 eV.

$$m_\nu^2 = -462 \pm 579_{(\text{stat})} \pm 679_{(\text{sys})}\, eV^2$$

$$\Downarrow$$

$$m_\nu < 26 \text{ eV } (95\% \text{ C.L.})$$

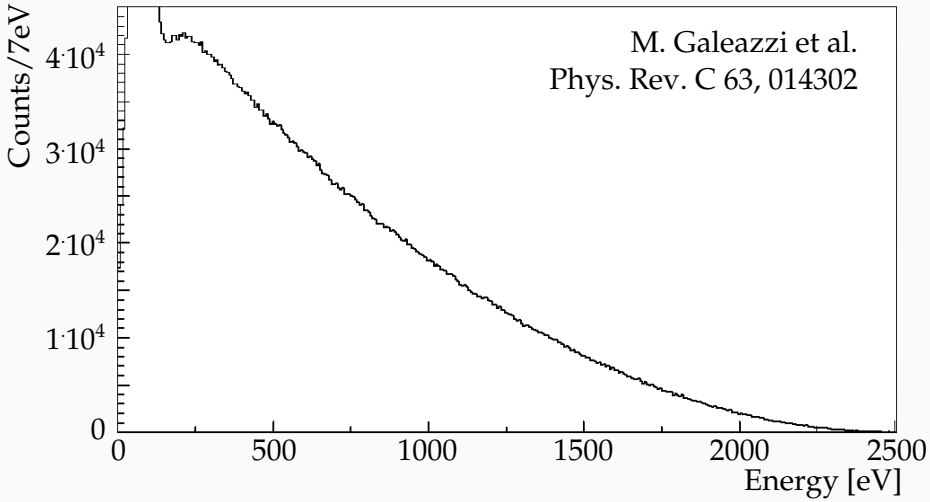

MIBETA (2002-2003)

- 10 $AgReO_4$ crystals: 2.71 mg;
- ^{187}Re activity: 0.54 Hz/mg;
- Sensor: Si thermistor (ITC-irst now FBK);
- Resolution: $\Delta E = 28.5$ eV FWHM;
- Live-time: 0.6 years;
- $6.2 \cdot 10^6$ ^{187}Re decays above 700 eV.

$$m_\nu^2 = -112 \pm 207_{(\text{stat})} \pm 90_{(\text{sys})}\, eV\, 2$$

$$\Downarrow$$

$$m_\nu < 15 \text{ eV } (90\% \text{ C.L.})$$

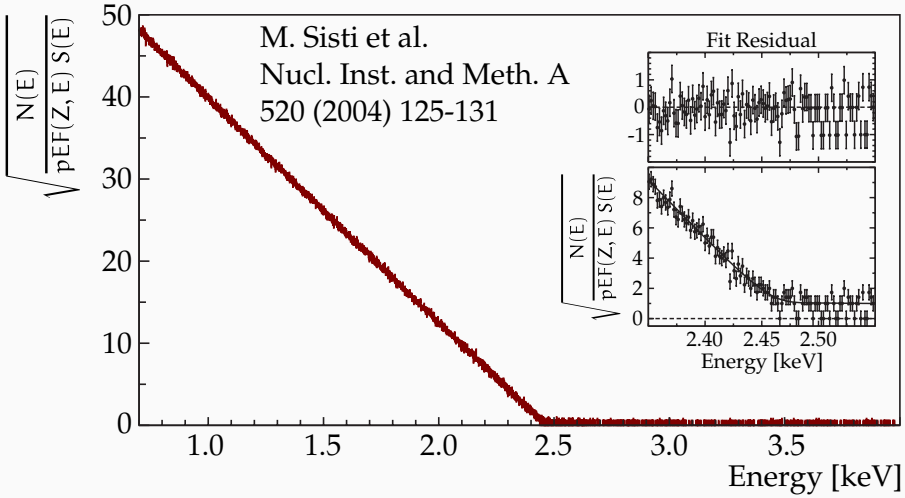

MARE: $AgReO_4$ with Si-implanted thermistors

- To improve the MANU and MIBETA limits a higher statistic is needed
  $\Rightarrow$ ^{187}Re embedded in large pixel arrays

- MARE-1 in Milan: Milano/FBK/Wisconsin/NASA
  (Nucl.Instrum.Meth. A559 (2006) 346-348)
  - 8 (6 $\times$ 6)-arrays of Si:P thermistors (NASA-GSFC) with $AgReO_4$ absorbers;
  - pixel size: (300 $\times$ 300 $\times$ 1.5 μm^3);
  - developed for X-ray spectroscopy with HgTe absorbers (ASTRO-E2);
  - target energy resolution: 25 eV @ 2.6 keV;
  - 288 sensors for a total of 10^{10} events;

- Single crystal of silver perrhenate ($AgReO_4$)
  - mass $\simeq$ 500 μg per pixel ($A_\beta \simeq$ 0.3 decay/sec);
  - regular shape (600 $\times$ 600 $\times$ 250 μm^3);
  - low heat capacity due to Debye law;

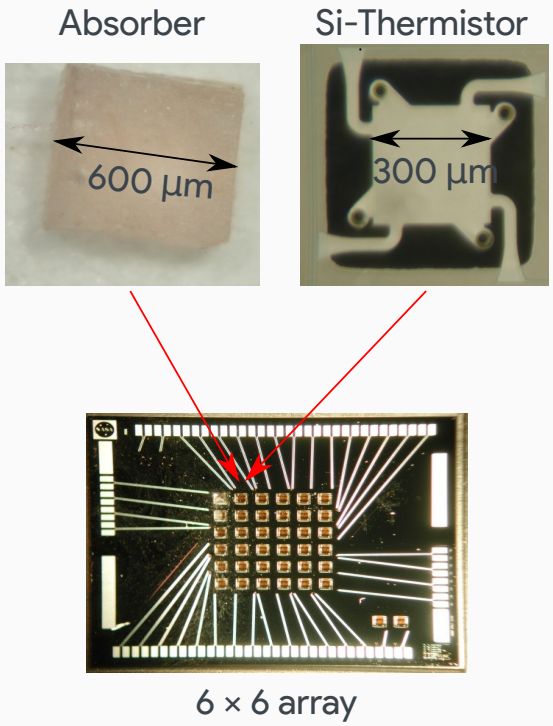

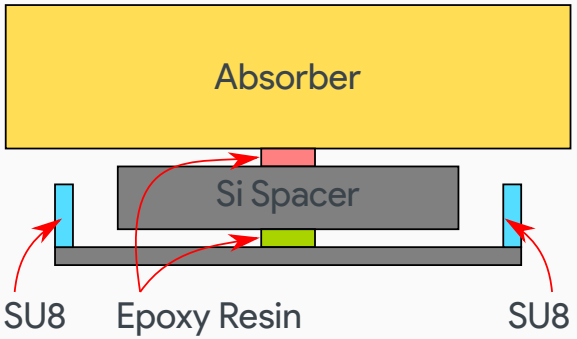

MARE: first results

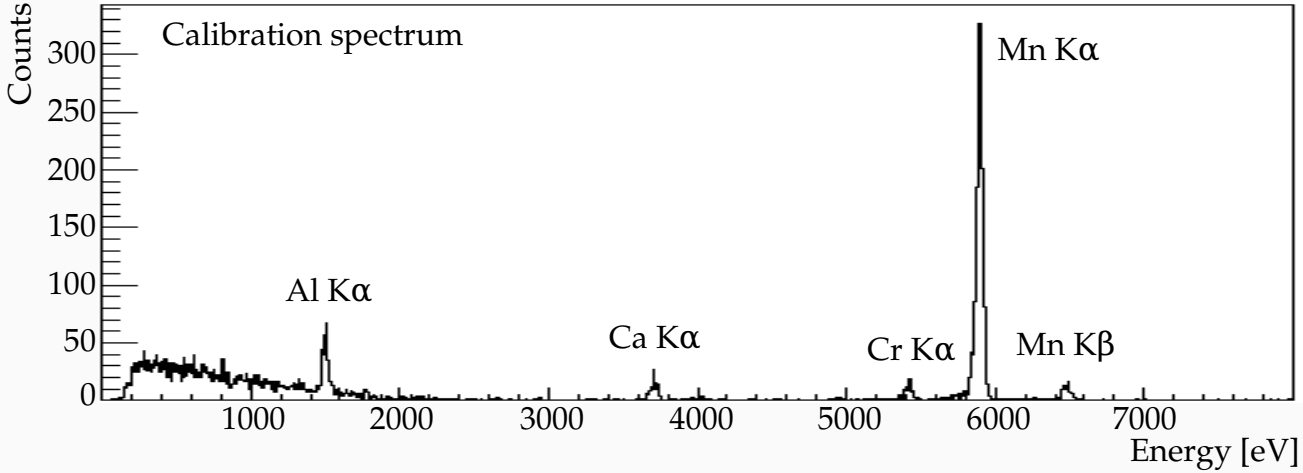

- 31 $AgReO_4$ crystals glued on 1st array;
- Only 16 usable: $\Delta E \simeq 47$ eV @ 2.6 keV, $\tau_{rise} \simeq$ 1 ms;
- Not enough for improving previous m_ν limits $\Rightarrow$ $m_\nu \leq 10$ eV in 1 year of live time.

J.Low.Temp.Phys. 176 (2014), 885-890

and

- No clear understanding of Re absorber physics;
- Extra thermal capacity C due to nuclear quadrupole moment?
- low specific activity $\Rightarrow$ need large mass to reach sub-eV sensitivity;
- systematics due to the Beta Environmental Fine Structure (BEFS);
- ... and due to the detector response function.

with the current technologies the future of Re experiments is not very bright

New approach: the EC of the ^{163}Ho

HOLMES

An interesting isotope suitable for the neutrino mass experiment is the ^{163}Ho.

$$^{163}\mathrm{Ho} + \mathrm{e}^- \rightarrow {}^{163}\mathrm{Dy}^* + \nu_e(E_c) \quad \text{electron capture from shell} > \mathrm{M1}$$

proposed by A. De Rujula e M. Lusignoli in 1982

(Phys.Lett. 118B (1982) 429 and Nucl. Phys. B219 (1983) 277-301)

- Calorimetric measurement of Dy atomic de-excitations (mostly non-radiative):
  - ⇒ measurement of the entire energy released except the ν energy;
- Lower is the Q-value higher is the rate at end-point;
- Q_{EC} and atomic de-excitation spectrum poorly known:
  - ⇒ Measured $Q_{EC} = 2.833$ keV with Penny Trap mass spectroscopy (Phys. Rev. Lett. 115 (2015) 062501);
  - ⇒ But no calorimetric measurements with enough statistics at the end point;
- $\tau_{1/2} \simeq 4570$ years ⇒ high specific activity:
  - ⇒ Holmium detector not needed;
  - ⇒ ^{163}Ho can be implanted in any suitable microcalorimeter absorber;
- Complex pile-up spectrum;
- Assessment of Q-value from the end-point of the calorimetric spectrum is a primary goal.

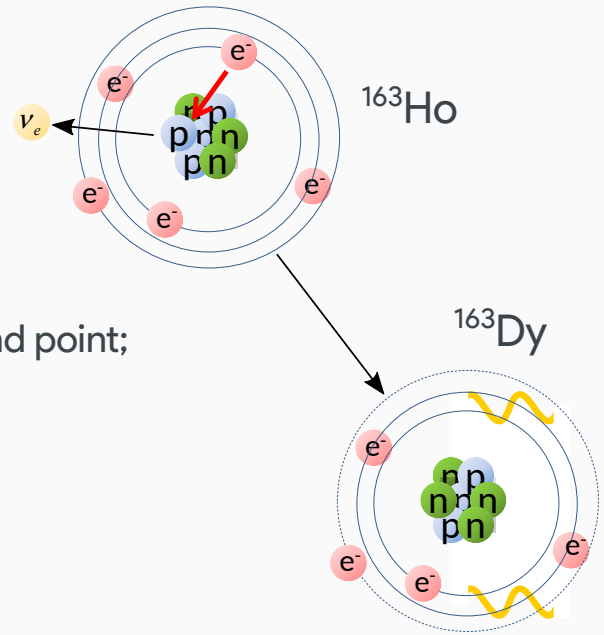

The ^{163}Ho EC spectrum

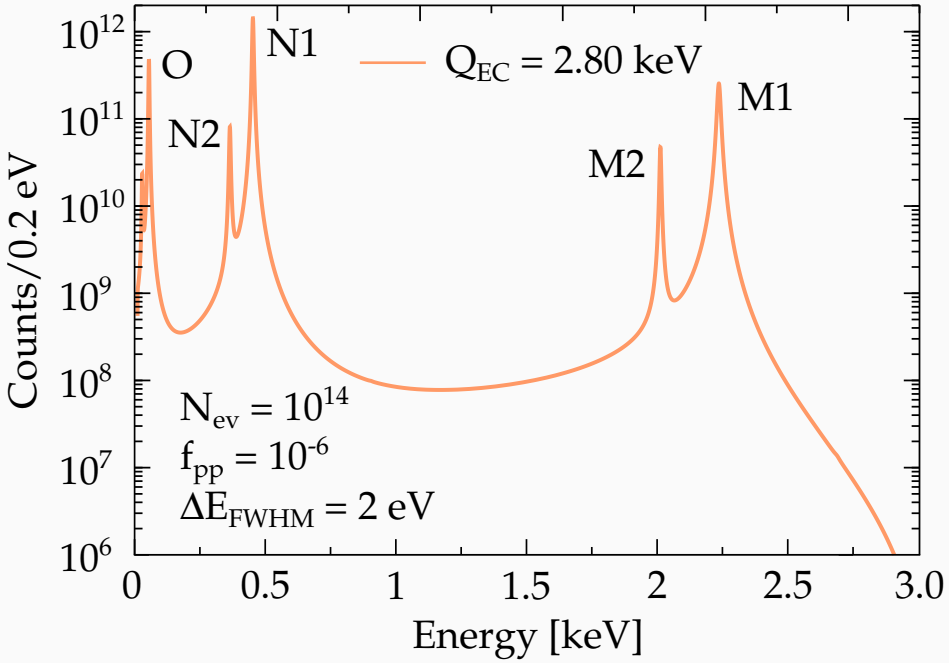

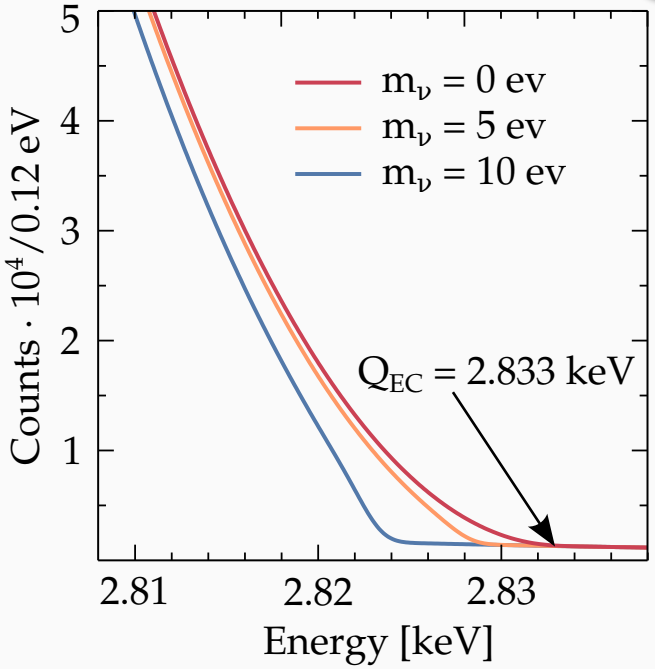

$$\frac{d\lambda_{\rm EC}}{dE_c} = \frac{G_\beta^2}{4\pi^2}(Q_{EC}-E_c)\sqrt{(Q_{EC}-E_c)^2-m_\nu^2}\cdot\sum_i n_i C_i \beta_i^2 B_i \frac{\Gamma_i}{2\,\pi}\frac{1}{(E_c-E_i)^2+\Gamma_i^2/4},$$

- Continuum with marked peaks with Breit-Wigner shapes lines (width Γ_i of a few eV);
- Series of lines at the ionization energies E_i of the captured electrons;
- End-point shaped by $(Q_{EC}-E_c)\sqrt{(Q_{EC}-E_c)^2-m_\nu^2}$ (the same of the β-decay);
- Self calibrating spectrum;

The ^{163}Ho EC pile-up spectra

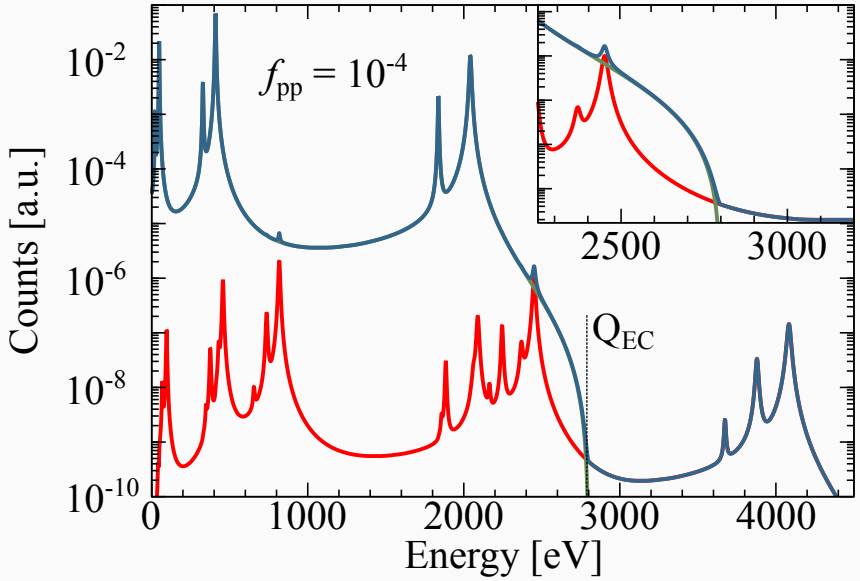

$$S(E_c) = \left[N_{ev}(N_{EC}(E_c, m_\nu) + f_{pp} \times N_{EC}(E_c, 0) \otimes N_{EC}(E_c, 0)) + B(E_c)\right] \otimes R_{\Delta E}(E_c)$$

A_{EC}	: decay activity
$f_{pp} = A_{EC} \times \tau_r$	: pile-up rate
$S(E_c)$	: total theoretical spectrum
$N_{EC}(E_c, m_\nu)$	: ^{163}Ho spectrum
$B(E)$	: background energy spectrum
$R_{\Delta E}(E_c)$	: detector energy response function

(more details in Eur. Phys. J. C 74 (2014) 3161)

- Pulse pile-up occurs when multiple events arrive within the temporal resolving time of the detector (i.e. $E_1 + E_2 = Q_{EC}$);
- Unresolved pile-up at the end-point Q_{EC} produces a sort of background close to the end-point;
- The ^{163}Ho pile-up events spectrum is quite complex and presents a number of peaks right at the end-point of the decay spectrum;
- To resolve pile-up:
  - Detector with hight time resolution τ_r (and fast signal rise-time τ_{rise});
  - Efficient pulse pile-up recovery algorithm (Wiener filter, Singular Value Decomposition)

The ^{163}Ho Potential sensitivity

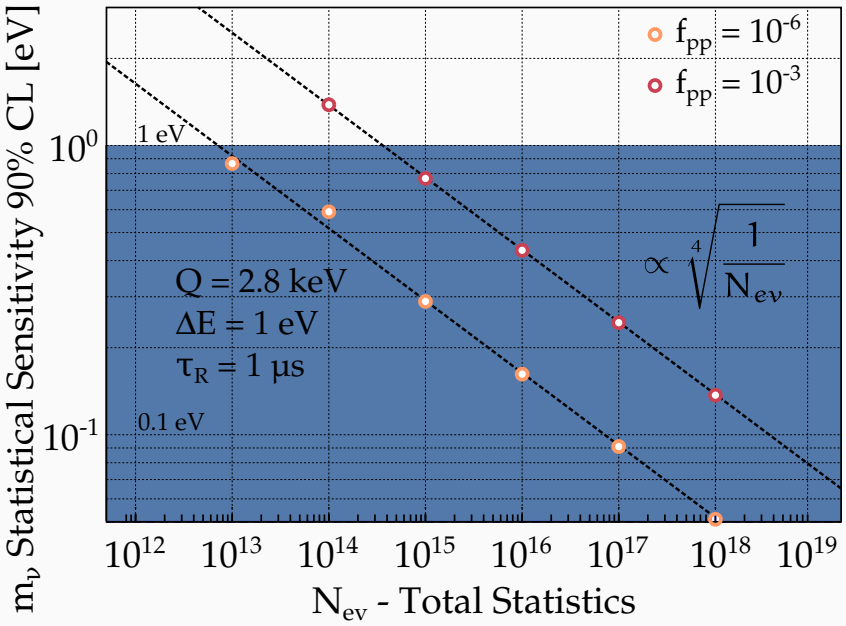

(plot from Adv. High En. Phys. 2016 (2016) 9153024)

$$m_\nu \leq 0.1\,\text{eV}: \begin{cases} A_{EC} = 1\,\text{Bq} \\ N_{det} \cdot t_{meas} \simeq 2 \cdot 10^9 \text{ det} \cdot \text{years} \\ \\ A_{EC} = 1000\,\text{Bq} \\ N_{det} \cdot t_{det} \simeq 10^8 \text{ det} \cdot \text{years} \end{cases}$$

The statistical sensitivity depends on:

- statistics: $N_{ev} = A_{EC} \cdot N_{det} \cdot t_{meas}$ ($m_\nu \uparrow$)
- pile-up fraction: $f_{pp} \simeq A_{EC} \cdot \tau_r$ ($m_\nu \downarrow$)

Requirements for $m_\nu \leq 0.1$ eV

- High energy resolution ($\simeq 1$ eV);
- Fast response detectors ($\simeq 1\,\mu$s) to avoid pile-up events;
- Multiplexable detectors array ($N_{pixel} > 1000$);

$\Downarrow$

Low Temperature Detector

$\Downarrow$

TESs, MMCs, MKIDs, ...

The ^{163}Ho Potential sensitivity: more MC simulations

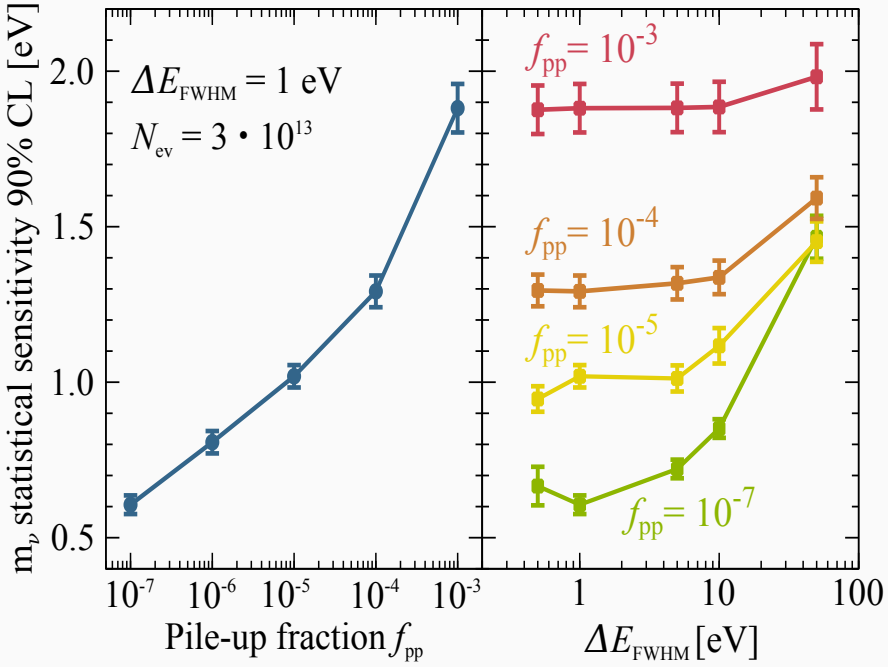

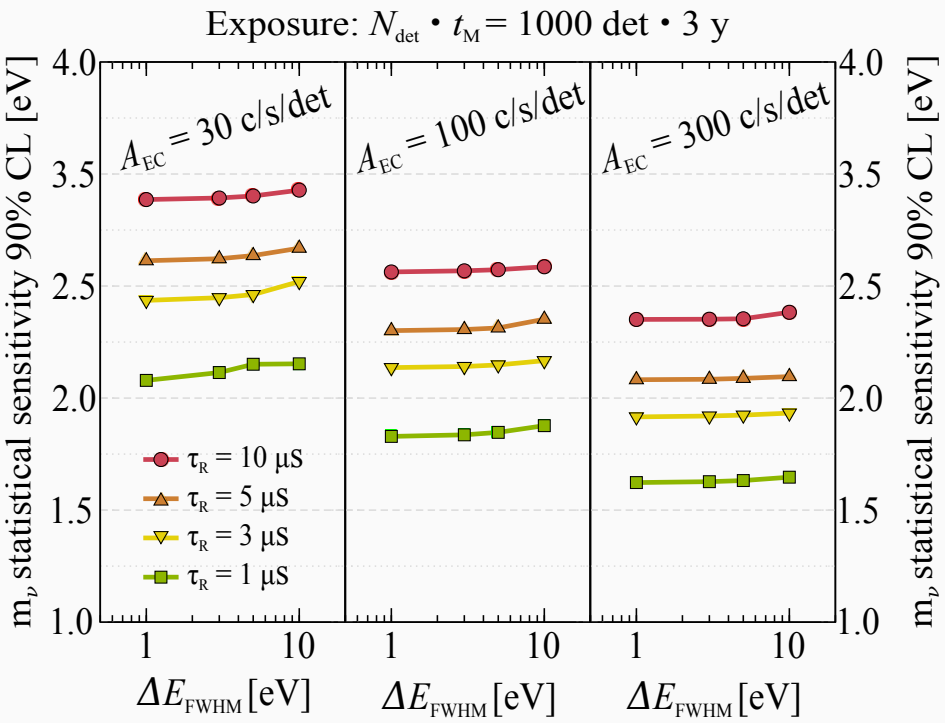

Statistical sensitivity m_ν dependencies from MC simulations:

- strong on the total statistics: $N_{ev} = A_{EC} \cdot N_{det} \cdot t_{meas} \Rightarrow m_\nu \propto N_{ev}{}^{1/4}$
- strong on rise time pile-up, probability: $f_{pp} \simeq A_{EC} \cdot \tau_R$ (with τ_R time resolution);
- weak on e nergy resolution ΔE.

Effect of background on sensitivity

HOLMES

Background sources:

- Environmental γ radiation:
  - Compton interactions;
  - Photoelectric interactions with photoelectron escape;
  - Fluorescent X-rays and X-ray escape lines;
- γs and βs from close surroundings;
- Cosmic rays at sea level (muons):
  - Au pixel: $200 \times 200 \times 3\ \mu m^3$ $\Rightarrow$ $E \simeq 10$ keV, rate $\simeq 1\ d^{-1}$;
  - Si chip: $20 \times 20 \times 0.5\ mm^3$ $\Rightarrow$ $E \simeq 300$ keV, rate $\simeq 7000\ d^{-1}$;

Experimental results:

- MIBETA: $300 \times 300 \times 150\ \mu m^3$ $AgReO_4$ crystals: $\Rightarrow$ $b(2.5keV) \simeq 1.5 \cdot 10^{-4}$ c/eV/d/det;
- TES @NIST (1600m): $350 \times 350 \times 2.5\ \mu m^3$ Bi absorbers: $\Rightarrow$ $b < 1$ c/eV/d/det (preliminary);

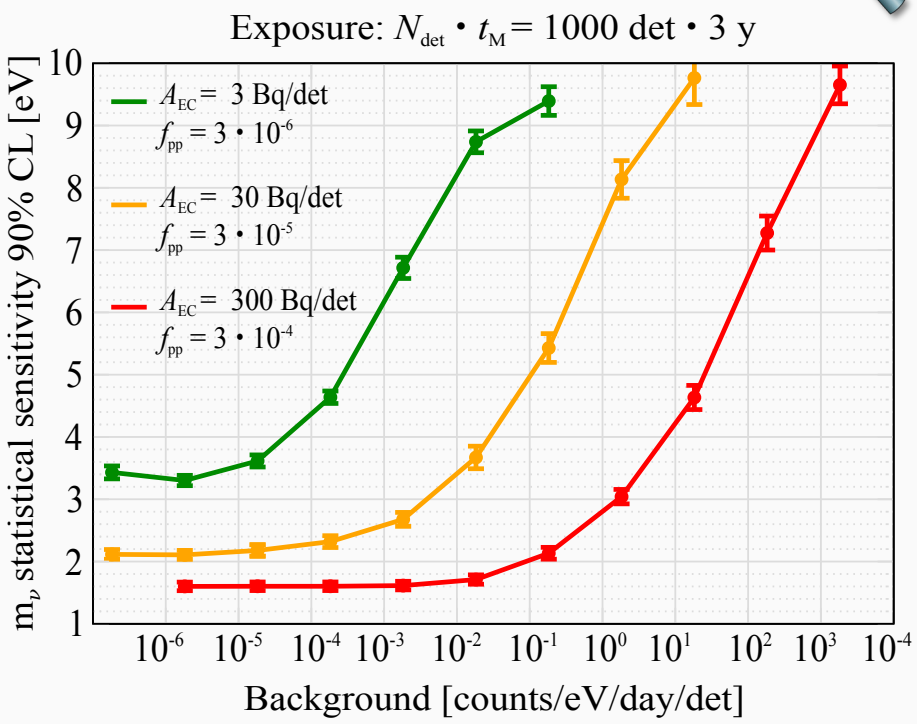

A constant background b is negligible if it is much smaller than the pile-up spectrum

$$b << \frac{A_{EC} \cdot f_{pp}}{2Q_{EC}}$$

If the pixel activity $A_{EC} \uparrow \Rightarrow$ the pile-up rate $f_{pp} \uparrow \Rightarrow m_\nu$ relatively insensitive to b.

^{163}Ho microcalorimeter experimental status

HOLMES

^{163}Ho seems to be better than ^{187}Re

- Higher specific activity ⇒ Holmium detector not needed;
- Self calibrating ⇒ better systematics control;
- ... but Atomic de-excitation spectrum poorly known;
- ... and complex pile-up spectrum;

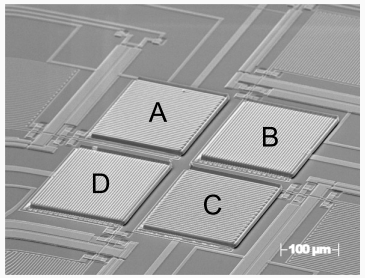

ECHo

Microcalorimeter projects with ^{163}Ho:

- ECHo, MMC detectors (Heidelberg, ...)
- NuMECS, TES detectors (LANL, NIST, ...)
- HOLMES, TES detectors (UNIMIB, INFN, NIST, ILL, PSI, ...)

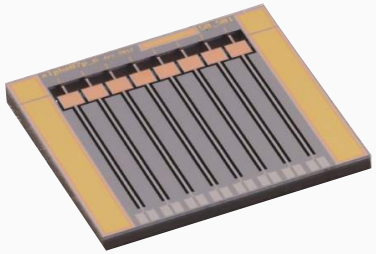

NuMECS

Common technical challenges:

- Clean ^{163}Ho production;
- ^{163}Ho incorporation;
- Large channel number ⇒ high speed multiplexing;
- Data handling (processing, storage, ...)

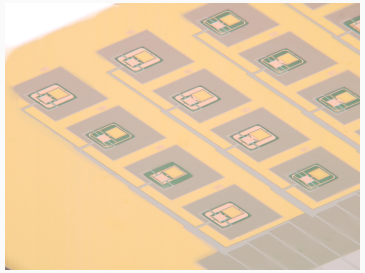

HOLMES

HOLMES

First detector prototype

- low temperature metallic magnetic calorimeters;
- embedding of ^{163}Ho source
  - ions production @ILL (Grenoble, France);
  - ions implantation @ISOLDE-CERN;
- about 0.1 Bq per pixel (MMC-ECHo-1);
- two pixels simultaneusly measured;

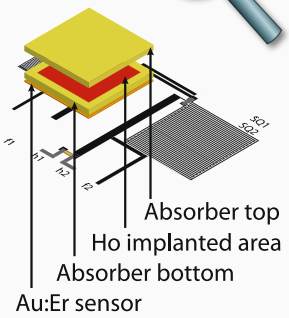

Calorimetric spectrum

- rise time $\tau_r \simeq 130$ ns;
- $\Delta E_{FWHM} = 7.6$ eV @ 6 keV;
- non-linearity $<1\%$ @ KeV;
- presently most precise ^{163}Ho spectrum;

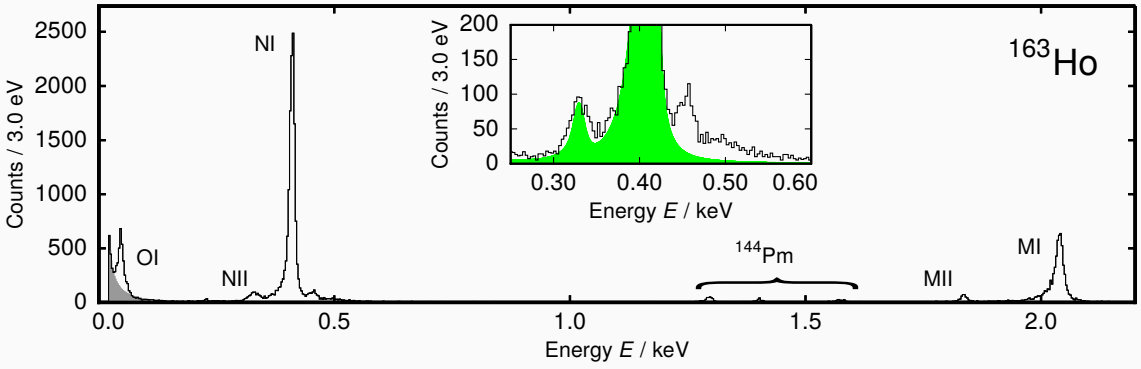

More details on
Phys. Rev. Lett. 119 (2017) 122501
Eur. Phys. J. ST 226 (2017) 1623-1694

ECHo-1k (2015 – current)

- Activity per pixel: 5 Bq
- Number of detectors: 60
- Readout: parallel two stage dc-SQUID
- Sensitivity: $m_\nu \simeq 10$ eV

ECHo-100k (2018 – 2021)

- Activity per pixel: 10 Bq
- Number of detectors: 12000
- Readout: microwave SQUID multiplexing
- Sensitivity: $m_\nu \simeq 1.5$ eV

HOLMES

First detector prototype

- Transition Edge Sensors;
- Embedding of ^{163}Ho source
  - proton irradiation of natural Dy @LANL Isotope Production Facility (IPF);
  - drying of solution containing ^{163}Ho onto thin nanoporous Au foil;
  - nanoporous gold foil doposited on regural Au;
  - absorber obtanied by folding and pressing a small piece of the Au foil;
- About 0.1 Bq per pixel;

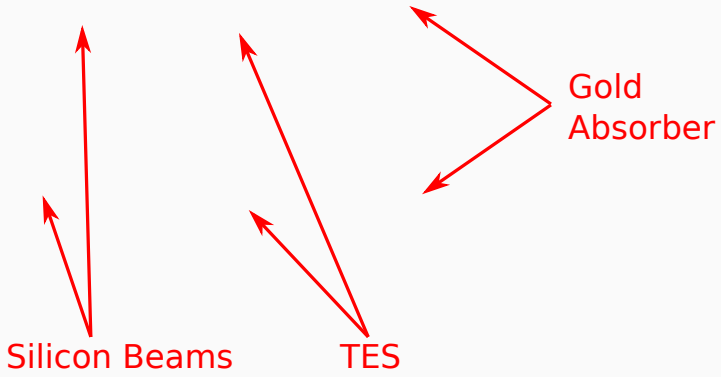

Calorimetric spectrum

- 40 hours measurement;
- ^{163}Ho spectrum with limited statistic;

Future developments

- 4×1024 pixel arrays;
- 100 Bq/pixel;
- Sensitivity: $m_\nu < 1$ eV after 1 year;

More details on
NuMECS Position Paper
J. Low. Temp. Phys. 184 (2016) 958-968

HOLMES (ERC-Advanced Grant n. 340321)

HOLMES

Goal

- Prove technique potential and its scalability
  $\Rightarrow$ baseline for a future Megapixel experiment;
- Neutrino mass measurement:
  $\Rightarrow$ statistical sensitivity $m_\nu < 2$ eV;
- Assess EC Q-value with a long calorimetric measurement;
- Assess systematic errors;

Baseline

- Transition Edge Sensors (TES) with ^{163}Ho implanted Au absorbers;
- $6.5 \cdot 10^{13}$ nuclei/detector (18 μg in total) $\Rightarrow$ 300 dec/s/pixel;
- $\Delta E \simeq (2-5)$ eV and $\tau_{rise} \simeq 10$ μs;
- 64-channel demonstrator/1024-channel final array;
- $3 \cdot 10^{13}$ events in 3 years of data taking;

Project Start: 1 Feb 2014

B. Alpert *et al.*, Eur. Phys. J. C75 (2015) 112

website: https://holmes0.mib.infn.it/holmes

HOLMES: ^{163}Ho production by neutron activation

HOLMES

Neutron activation of enriched ^{162}Er

$^{162}\mathrm{Er}(n,\gamma)^{163}\mathrm{Er}$ $\qquad \sigma_{therm} = 20\,\mathrm{b}$

$^{163}\mathrm{Er} \rightarrow {}^{163}\mathrm{Ho} + \nu_e \qquad \tau_{EC}^{1/2} = 75\,\mathrm{min}$

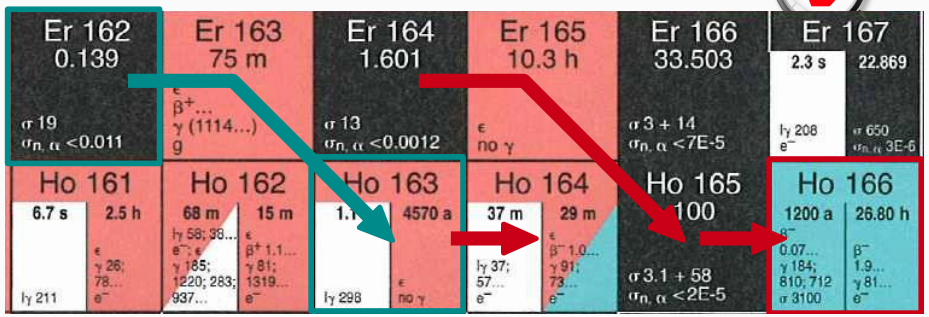

- ^{132}Er irradiation at ILL (Institut Laue-Langevin) nuclear reactor (Grenobsobtole, France);
  - ⇒ Thermal neutron flux at ILL: $\Phi_n = 1.3 \cdot 10^{15}\ \mathrm{n/cm^2/s}$;
  - ⇒ Cross section burn up $^{163}\mathrm{Ho}(n,\gamma)^{164}\mathrm{Ho}$ not negligible ($\simeq 200\,\mathrm{b}$)
  - ⇒ Unavoidable $^{165}\mathrm{Ho}(n,\gamma)^{166m}\mathrm{Ho}$, mostly from $^{164}\mathrm{Er}(n,\gamma) \rightarrow {}^{166m}\mathrm{Ho}\ (\beta^- : \tau_{1/2} = 1200\,\mathrm{y})$:
    $\Rightarrow A(^{163}\mathrm{Ho})/A(^{166m}\mathrm{Ho}) = 100 - 1000$

- Chemical pre-purification and post-separation at Paul Scherrer Institute (based on ion exchange chromatography) leaves a 166:163 ratio better than 1:1000 (PLoS ONE 13 (2018) e0200910)

- Thermoreduction to obtain the metallic Ho target for implantation.
  - ⇒ $\mathrm{Ho_2O_3} + 2\mathrm{Y}(met) \rightarrow 2\mathrm{Ho}(met) + \mathrm{Y_2O_3}$ @ 2000°C

- HOLMES needs $\simeq 200$ MBq of ^{163}Ho.

- 540 mg of 25% enriched $\mathrm{Er_2O_3}$ irradiated 50 days at ILL in 2017 (separation in progress);
  - ⇒ $A(^{163}\mathrm{Ho})_{theo} \simeq 100$ MBq ⇒ enough for R&D and 512 pixels
    $A(^{166m}\mathrm{Ho}) \simeq 180$ kBq.

HOLMES: mass separation and ion implanter

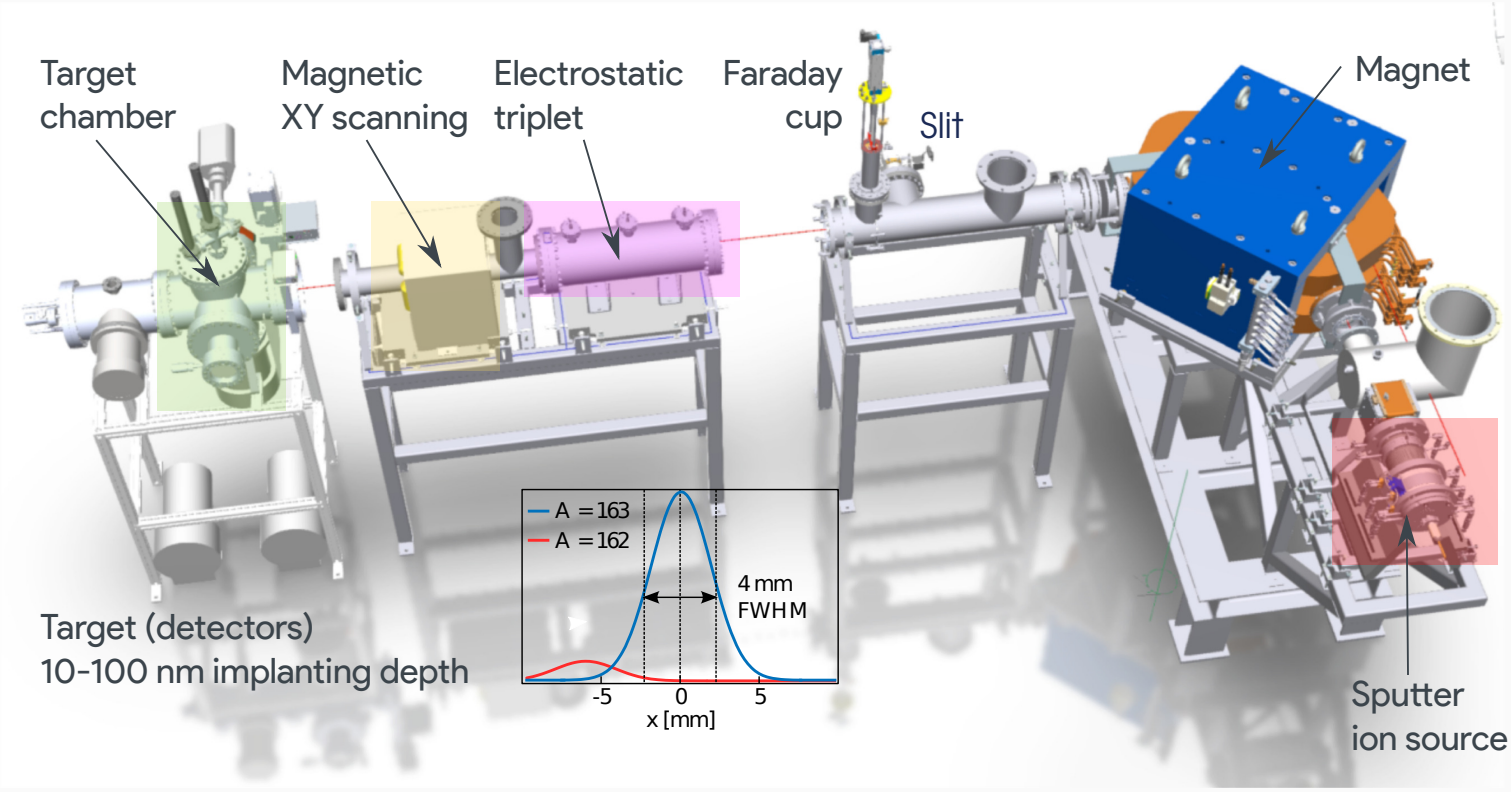

- Argon penning sputter ion source with an acceleration section allowing to reach a maximum energy of 50 keV;
- Magnetic dipole mass analyzer with magnetic field up to 1.1 T;
- Focusing electrostatic triplet and magnetic scanning stages;
- From MC simulations $\Rightarrow$ beam spot $\sim$ 4 mm FWHM at the target chamber;
- Expected 163/166*m* separation $\geq 5\sigma$.

More details on
J. Low Temp. Phys. (*in press*)
NIMA (*in press*)

HOLMES: mass separation and ion implanter (cont.)

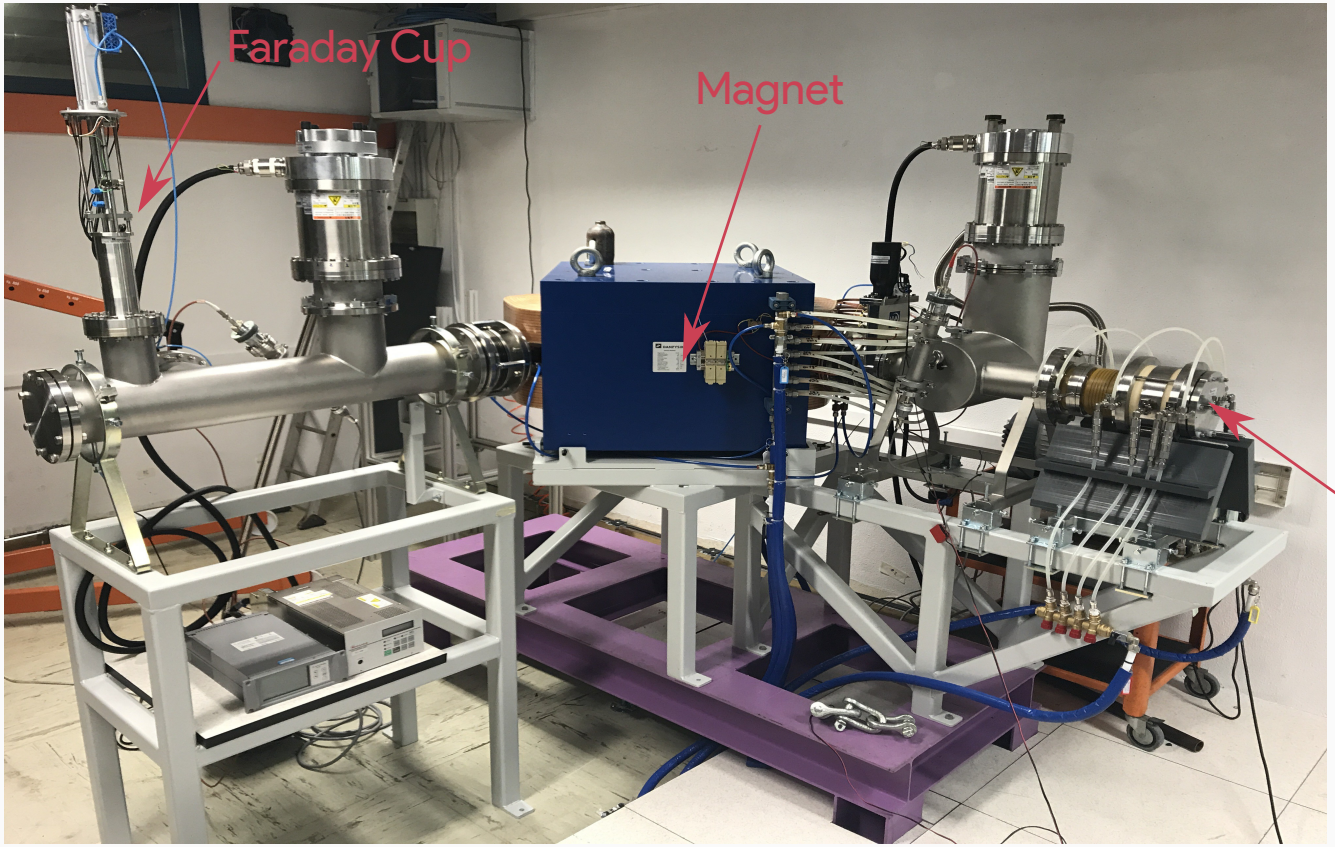

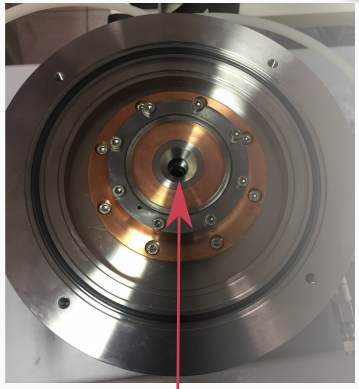

Sputter ion source

- Ion implanter currently in comissioning phase in INFN-Genova laboratory;
- Test in progess without focussing and with ^{nat}Ho as targer source;
- Triplet and scanning stages ready to be installed.
- ^{163}Ho implanting activity will be optimized during 2019.

HOLMES: deposition and target chamber

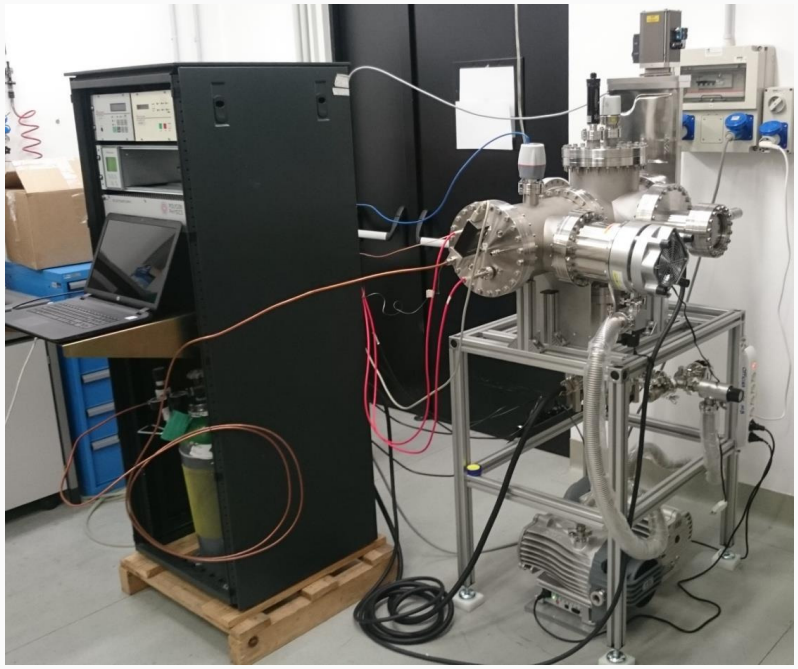

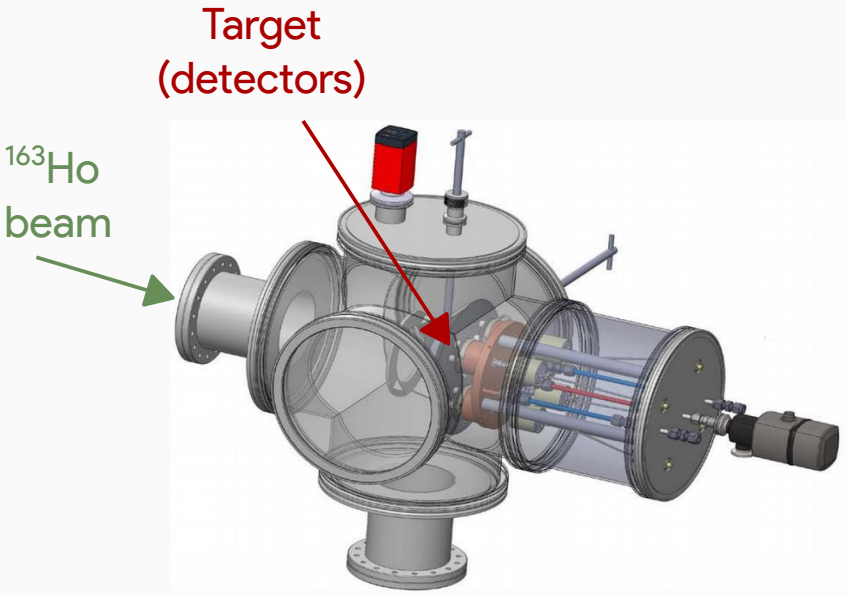

- To obtain $A_{EC} = 300$ Bq/det, the ^{163}Ho concentration in absorbers saturate because ^{163}Ho sputters off Au from absorber;
- Effect compensated by Au co-evaporation during the implantation procedure;
- Absorbers finalization with 1 μm Au layer deposited in situ to avoid oxidation;
- Au deposition rate $\sim$ 100 nm/hour (tunable with RF power or with Ar energy);
- Currently under comissioning at the University of Milano-Bicocca;

HOLMES: TES-based microcalorimeters

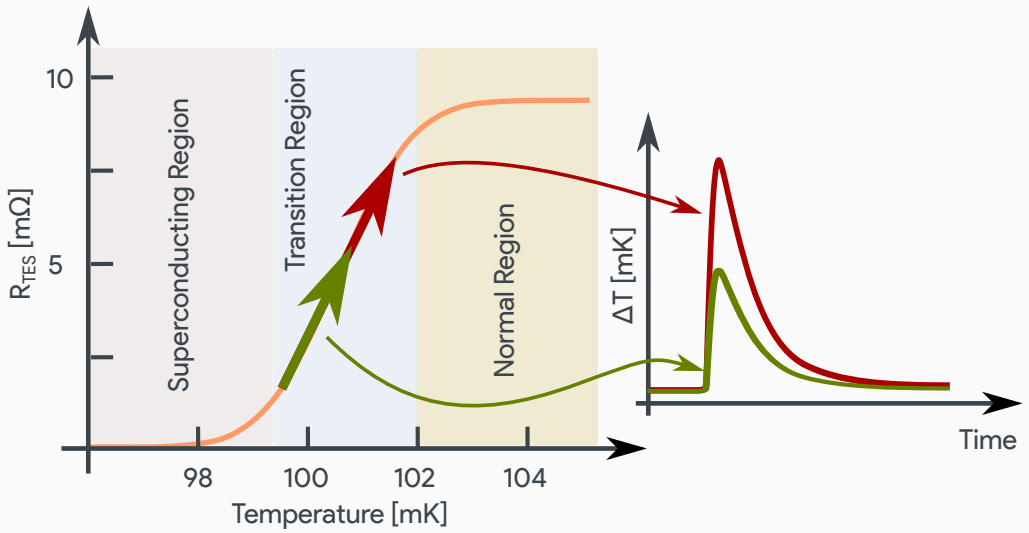

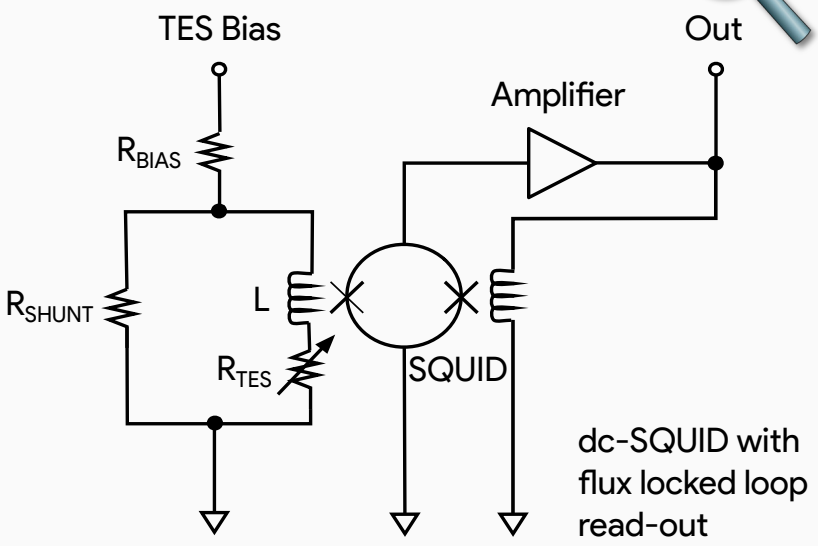

- Superconductor biased in its transition ⇒ strongly temperature-dependent resistance;
- "Self-biased region" ⇒ the power dissipated in the device is constant with the applied bias;
  - Electrothermal feedback: if $R_{TES} \uparrow \Rightarrow I_{TES} \downarrow \Rightarrow P_J \downarrow$ ⇒ cooling the device back to its equilibrium state in the self-biased region;
- Low resistance: read out with SQUIDs (Superconducting Quantum Interference Devices);
  - TES operates in series with the input coil L which is inductively coupled to the SQUID:
  - Change in TES current ⇒ change in the input flux to the SQUID;
- SQUIDs enable multiplexing ⇒ read out of many sensors using a smaller number of amplifier channels

HOLMES: Why TESs?

- Strongly supported by the X-ray astrophysics community for the past couple of decades (but also Dark Matter and rare events research);
- Small size $\Rightarrow$ low thermal capacity C $\Rightarrow$ excellent energy resolution:

$$\Delta E_{FWHM} = \begin{cases} 1.26\ \text{eV} \ @\ 1.5\ keV \\ 1.58\ \text{eV} \ @\ 6\ keV \\ 1.94\ \text{eV} \ @\ 8\ keV \end{cases}$$

- The negative electro-thermal feedback provides a fast time response;
- Large array
- Cross-talk between pixels less than 0.01%;
- Tunable critical temperature T_C exploiting the proximity effect $\Rightarrow$ Mo/Au or Mo/Cu proximity TES ($T_C \simeq 100$ mK);

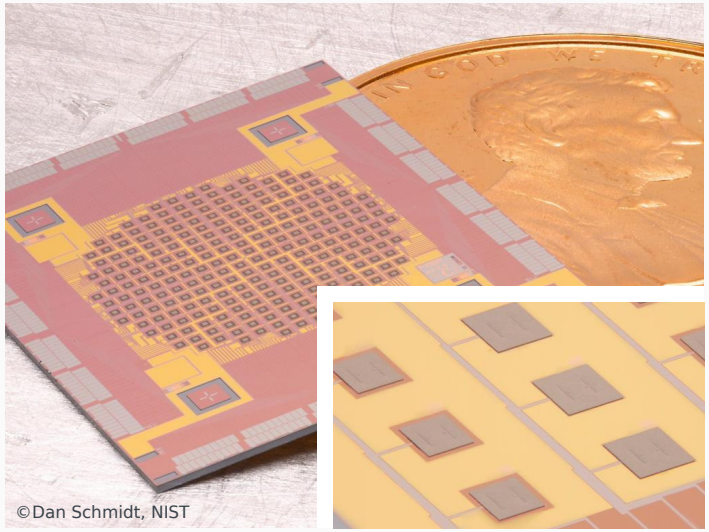

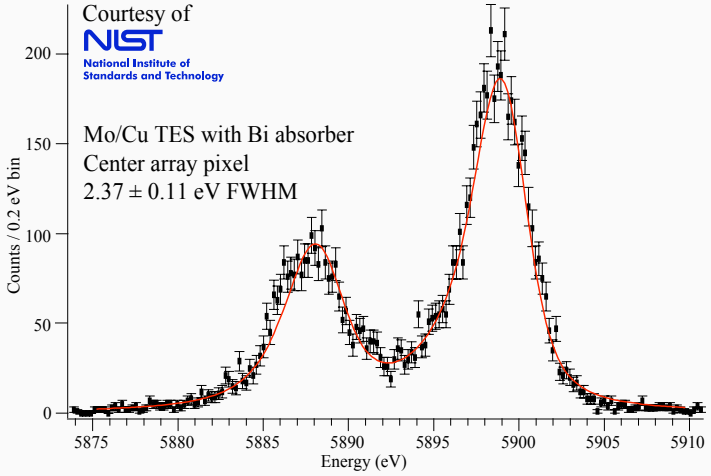

NIST design is the starting point for the HOLMES array detector

HOLMES: TESs design

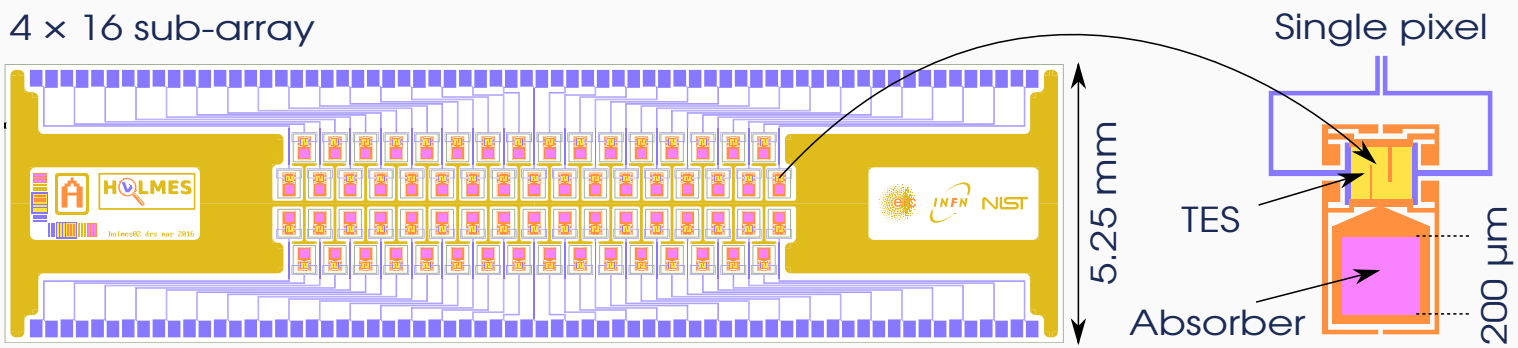

- Sensor: TES Mo/Au bilayers, critical temperature $T_c = 100$ mK;
- Absorber: Gold, 2 μm thick for full e/γ absorption;
- Side-car design to avoid TES proximitation;
- Thermal conductance G engineering for τ_{decay} control;
- 4×16 linear sub-array designed for high implant efficiency;
- Optimized design for high speed and high resolution:

$$@3\,\text{keV} : \Delta E_{FWHM} \simeq 3 - 4\,\text{eV}\,,\ \tau_{\text{rise}} \simeq 10\,\mu\text{s}\,,\ \tau_{\text{decay}} \simeq 100\,\mu\text{s}$$

HOLMES: TESs fabrication

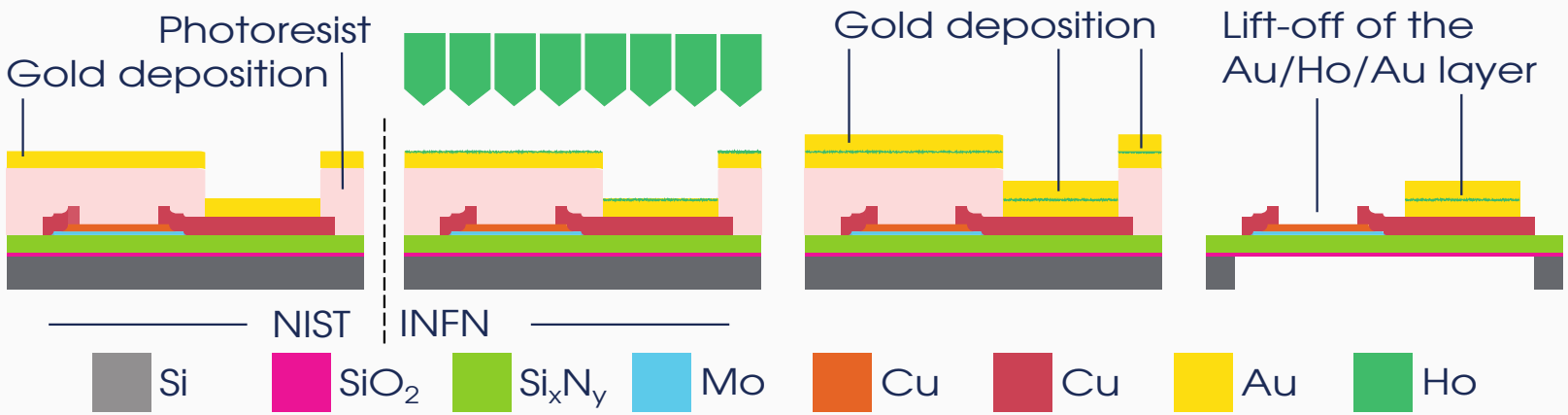

- Fabrication in two steps:
  - NIST: Au absorber bottom-part placed side-by-side with the Mo/Cu sensor on a silicon nitride;
  - INFN: Au absorber finalized into the implanter deposition chamber during the ^{163}Ho implanting procedure;
- SiN membrane release by Silicon Deep Reactive Ion Etching (DRIE) or Silicon KOH anisotropic wet etching $\Rightarrow$ tests currently in progress;
- 2 μm thick Au encapsulating implanted Ho;

HOLMES: the need for speed

- Many current and future applications for TESs require:
  - significantly faster pulse response
  - large arrays ($N_{\text{pixels}} > 1000$)

- Neutrino endpoint (HOLMES) need enormous statistics:
  - $\Rightarrow$ large number of pixel (>1000);
  - $\Rightarrow$ high activity per pixel ($\sim$ 300 event/sec/pixel);
  - $\Rightarrow$ faster response to avoid pile-up effects (that can distort spectra)

- Detectors at free-electron laser facilities
  - $\Rightarrow$ pulse response fast enough to match repetition rates of the source;

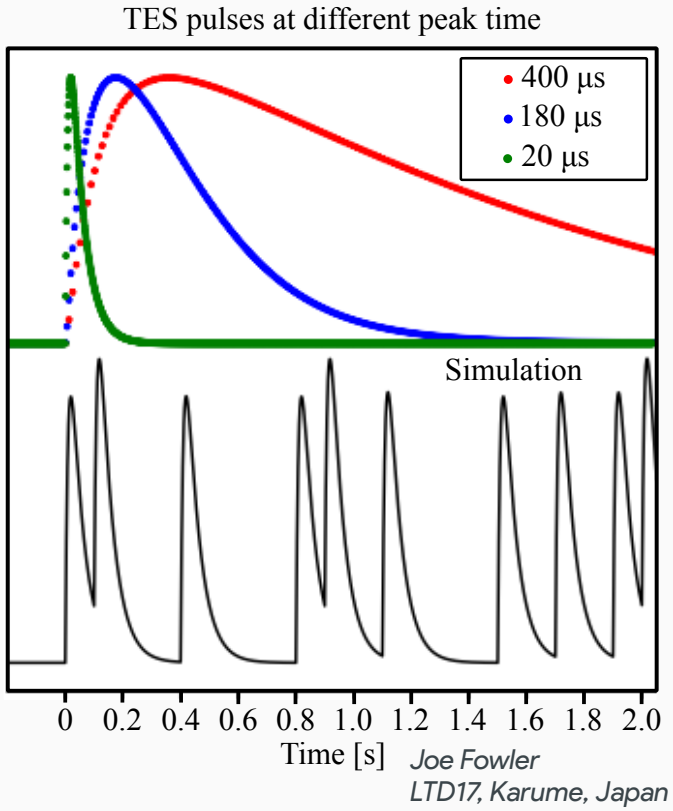

Joe Fowler
LTD17, Karume, Japan

- These applications need pulse times around 100 μs;

- A rapid pulse rise can facilitate the pile-up rejection but an adequate read out bandwidth is a fundamental requirement;

- The classical multiplexing schemas (TDM, CDM and FDM) provides a limited multiplexing factor (< 40) and limited bandwidth (few megahertz) on single detector.

Microwave rf-SQUID multiplexing

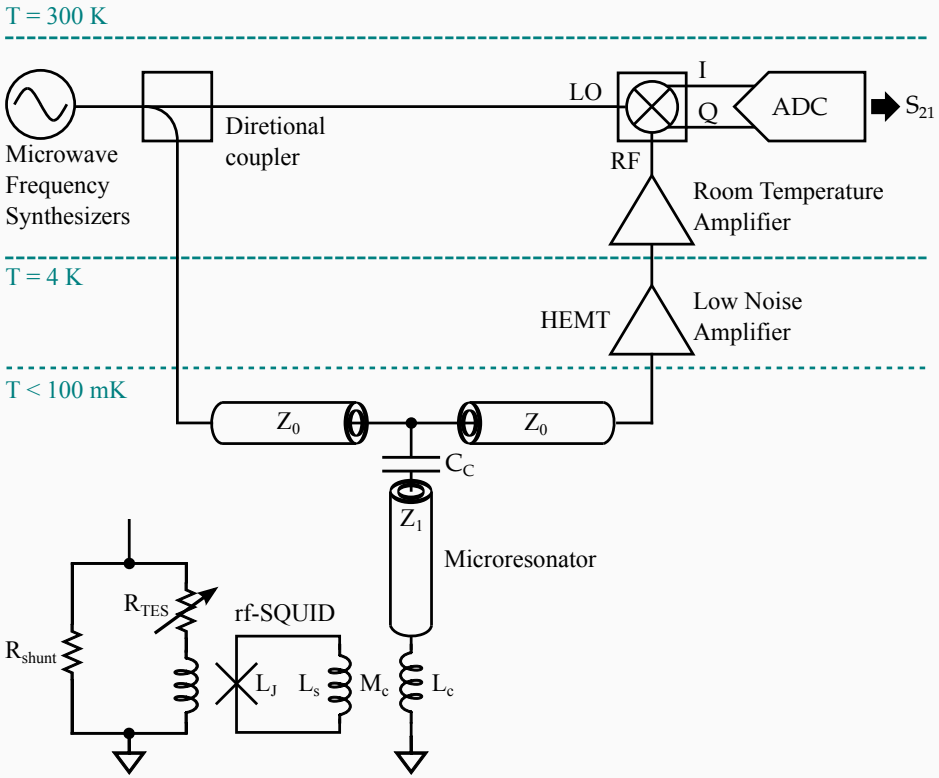

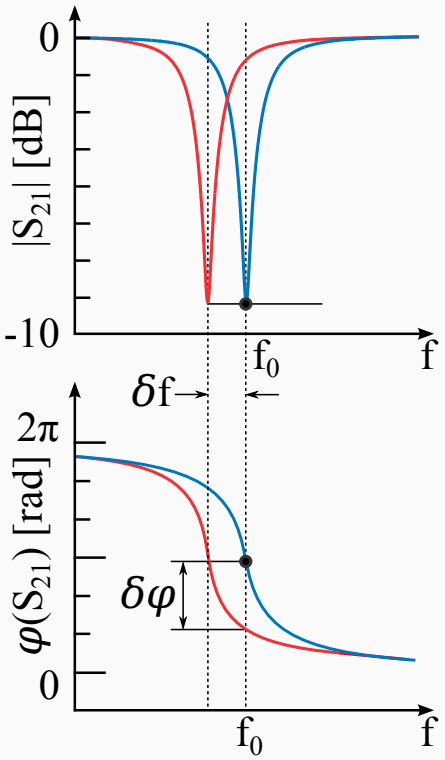

- dc-biased TES inductively coupled to a dissipationless rf-SQUID;
- rf-SQUID inductively coupled to a high-Q superconducting $\lambda/4$ resonator;
- Change in TES current $\Rightarrow$ change in the input flux to the SQUID;
- Change in the input flux to the SQUID $\Rightarrow$ change of resonance frequency and phase;
- Each micro-resonator can be continuously monitored by a probe tone;

Microwave rf-SQUID multiplexing (cont.)

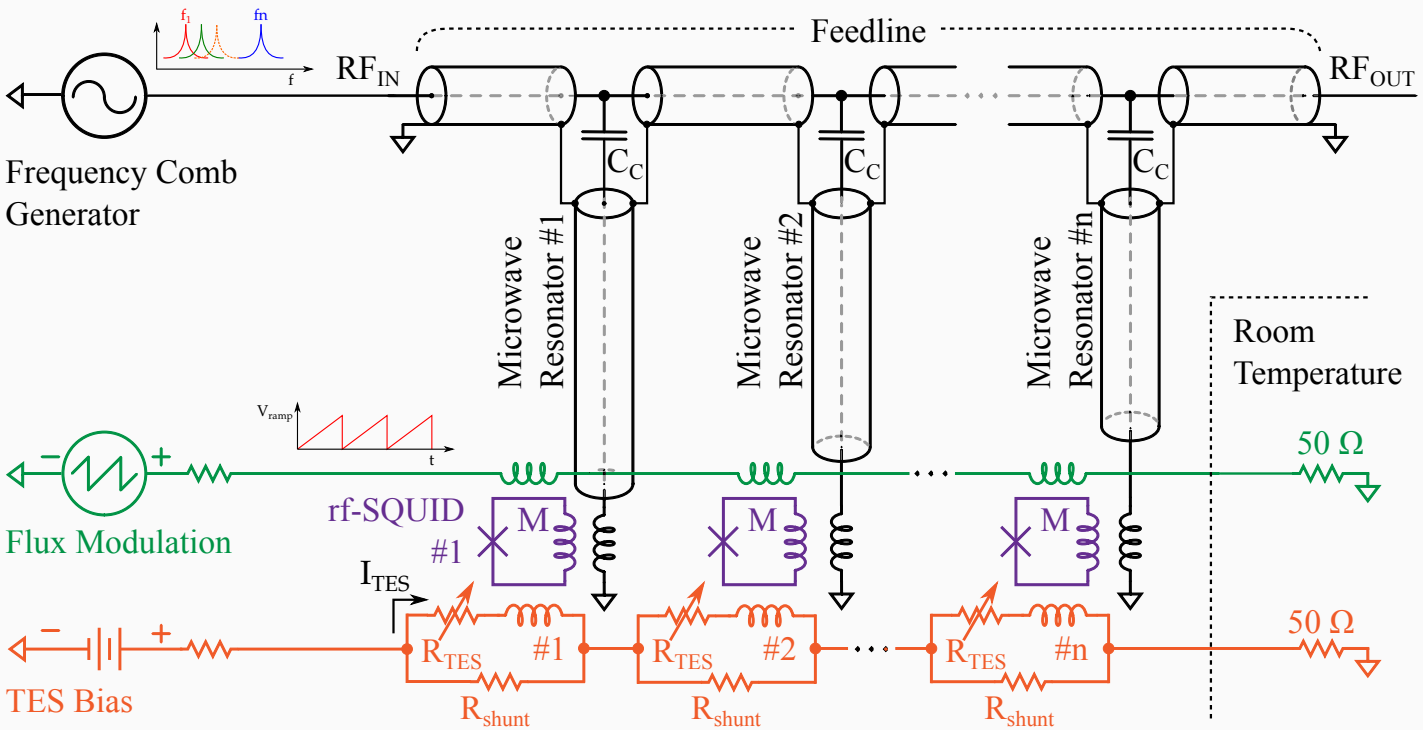

- By coupling many resonators to a single microwave feedline it is possible to perform the readout of multiple detectors
- Sensors are monitored by a set of sinusoidal probe tones (frequency comb);
- At equilibrium, the resonator frequencies are matched to the probe tone frequencies, and so each resonator acts as a short to ground;
- The ramp induces a controlled flux variation in the rf-SQUID, which is crucial for linearizing the response;
- Large multiplexing factor (> 100) and bandwidth, currently limited by the digitizer bandwidth.

The Multiplexing chip

The core of the microwave multiplexing is the multiplexer chip

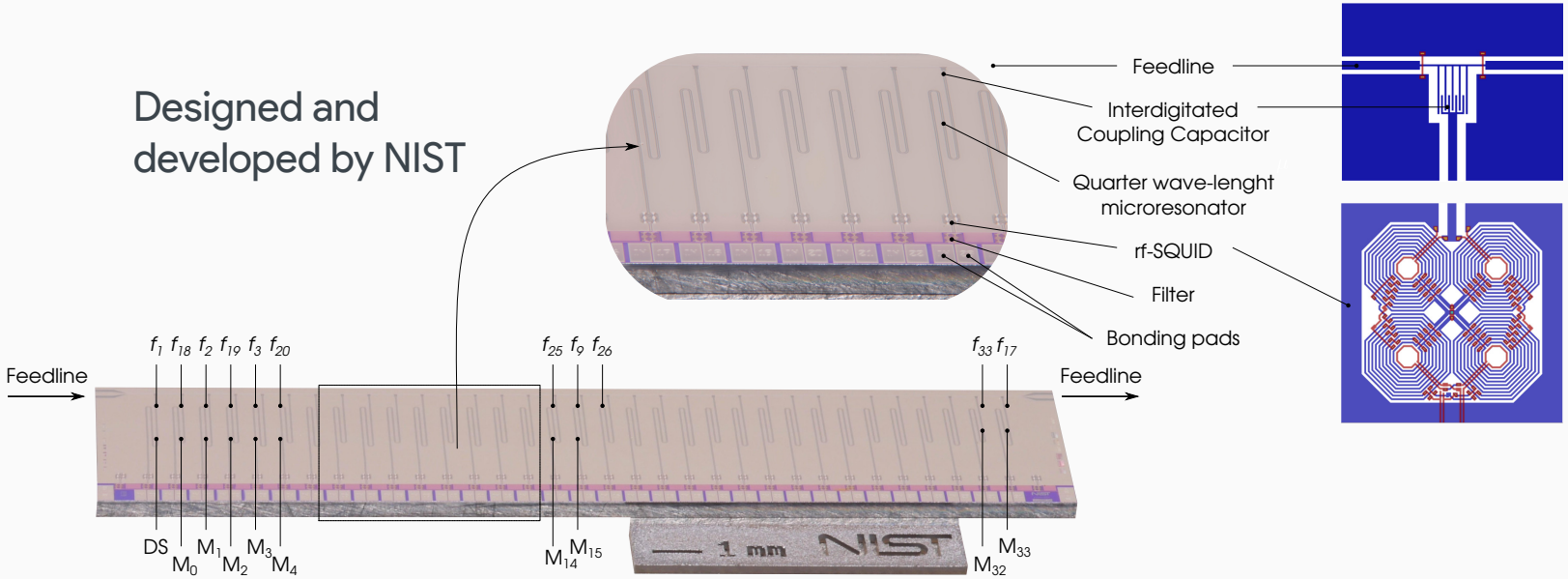

- Superconducting 33 quarter-wave coplanar waveguide (CPW) microwave resonators;
- 200 nm thick Nb film deposited on high-resistivity silicon ($\rho > 10\,\mathrm{k\Omega{\cdot}cm}$);
- Each resonator has a trombone-like shape with slightly different length;
- The SQUID loop is a second order gradiometer consisting of four parallel lobes;
- Wiring in series different 33-channel chips with different frequency band allows to increase the multiplexing factor (daisy chain)

Microwave readout hardware implementation

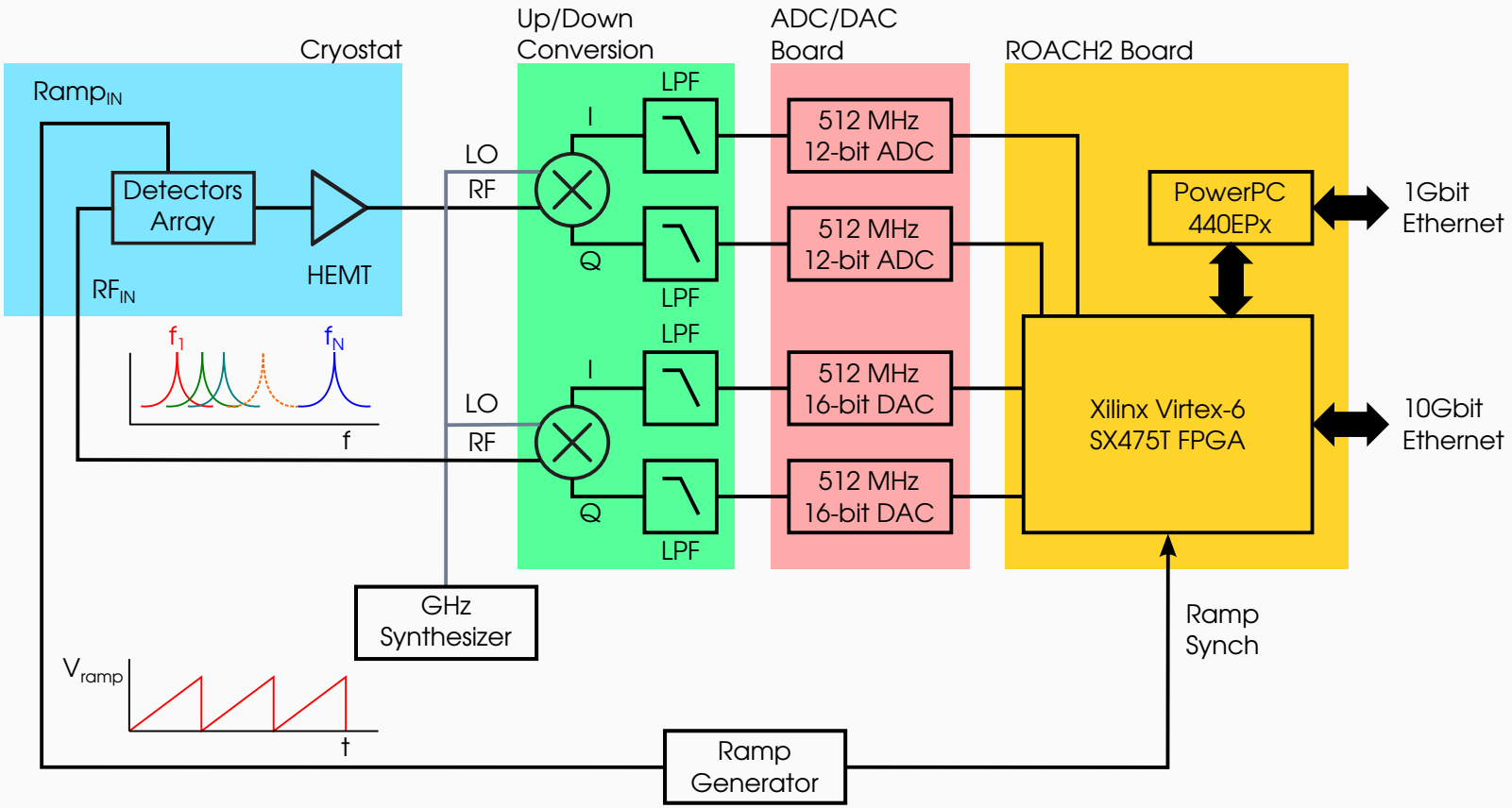

- A key enabling technology for large-scale microwave multiplexing is the digital approach;
- This allows to exploit standard software-defined radio (SDR) used in microwave-frequency communication.
- Open architecture computing hardware ROACH2 (Reconfigurable Open Architecture Computing Hardware) as FPGA processing board;

Bandwidth Budget and multiplexing factor

HOLMES

The number of multiplexable TESs per ADC board is

$$n_{\mathrm{TES}} = \frac{f_{\mathrm{ADC}} \cdot \tau_r}{2 \cdot n_{\Phi_0} \cdot g_f \cdot R_d} \quad \text{with} \quad \Delta f_{\mathrm{BW}} \geq 2\, f_r\, n_{\Phi_0} \quad , \quad S \geq g_f\, \Delta f_{\mathrm{BW}} \quad , \quad f_s = f_{\mathrm{ramp}} \geq \frac{R_d}{\tau_r}$$

f_s = sampling rate

f_{ramp} = flux ramp frequency

Δf_{BW} = resonator bandwidth

n_{Φ_0} = number of flux quantum per ramp

S = frequency spacing between tones

g_f = guard factor between tones

τ_r = rise time

R_d = distortion suppression factor (2 is Nyquist limit)

f_{ADC} = ADC bandwidth

n_{TES} = number of TES per board

The target rise time for HOLMES is $\tau_r = 10\ \mu s$

τ_r [μs]	f_r [kHz]	f_{ADC} [MHz]	n_{Φ_0}	Δf_{BW} [MHz]
10	500	500	2	2
g_f	S [MHz]	R_d	n_{TES}	
7	14	5	$\sim$36	

- The HOLMES multiplexing factor is around $\Rightarrow$ 32 pixels per ADC board;
- In order to cover the total 1024 pixels $\Rightarrow$ 1024/32=32 ADC boards are needed;
- The typical RF bandwidth for a HEMT amplifier is from 4 to 8 GHz;
  $\Rightarrow$ a single HEMT can amplify $\Rightarrow$ 4000 MHz/500 MHz=8 ADC boards;
- 4 HEMT amplifiers are needed for a total of $\Rightarrow$ 32 ADC boards;

HOLMES: 1st detectors generation

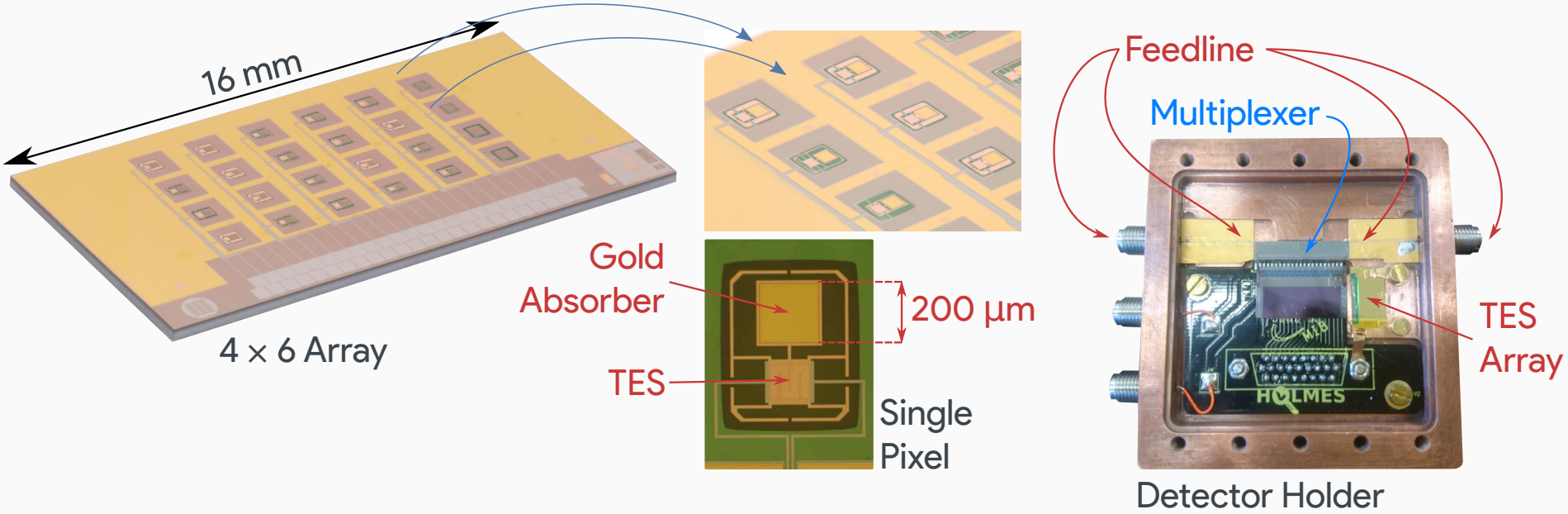

- Sensor: TES Mo/Au bilayers, critical temperature $T_c = 100$ mK;
- Absorber: Gold, 2 μm thick for full e^-/γ absorption (sidecar design);
- First 4 $\times$ 6 array prototype produced at NIST at test in Milano with μwave-readout;
- Different Perimeter/Absorber configurations in order to study the detector response;

HOLMES: multiplexer chip characterization results

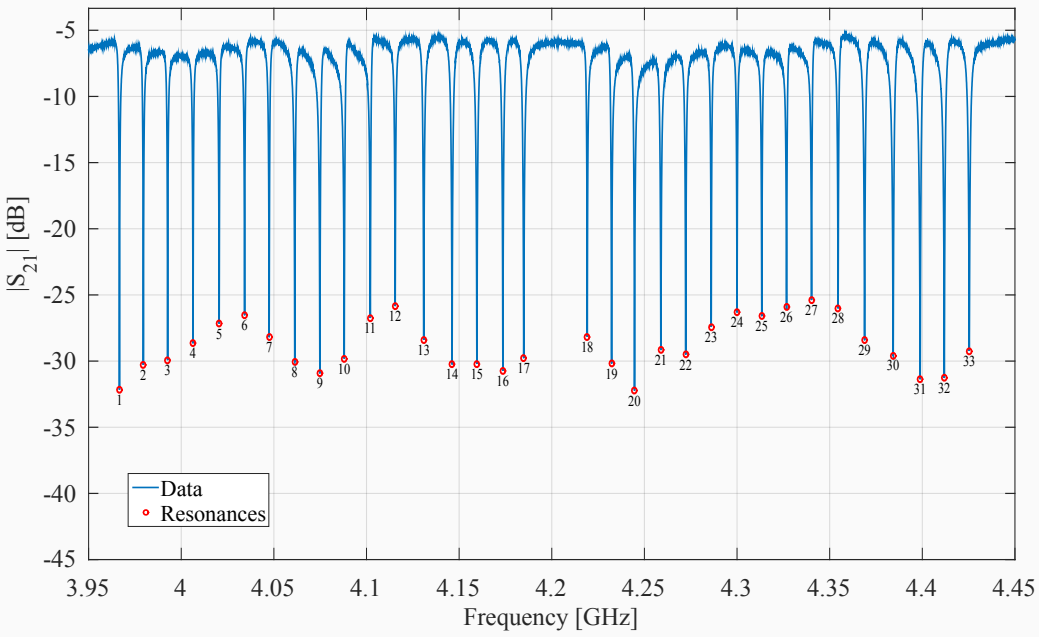

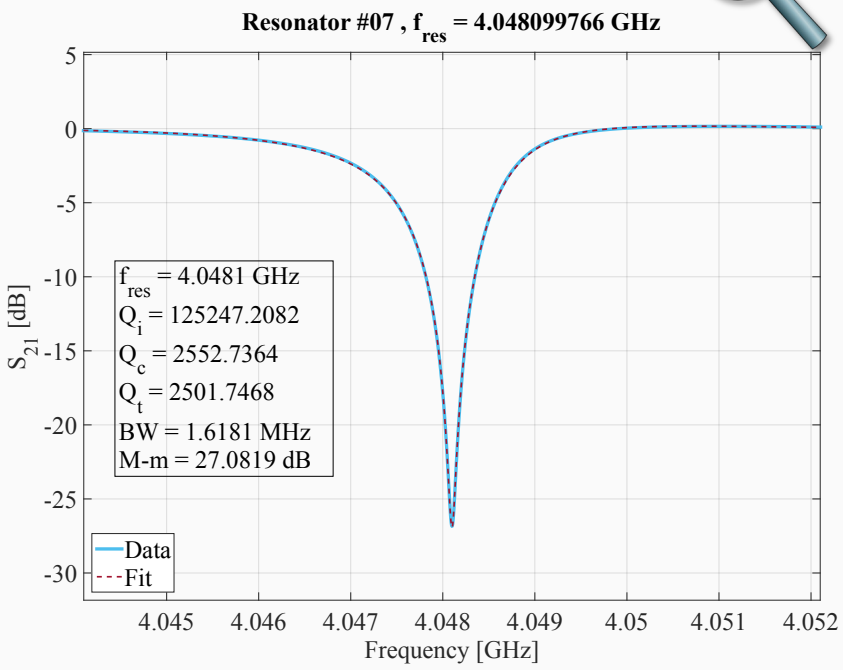

- Multiplexer μmux17a specifically optimized for HOLMES at NIST;
- New design for increasing the resonators uniformity;
- Characterization results confirmed the design specifications:
  - All 33 resonators present and usable for microwave readout;
  - Resonator bandwidth around: $\Delta f_{\mathrm{BW}} = 2\,\mathrm{MHz}$;
  - Frequency spacing between resonances around: $S = 14\,\mathrm{MHz}$;
  - Resonances depth $\geq 10\,\mathrm{dB}$;
  - SQUID noise: $n_{\mathrm{SQUID}} \leq (2-3)\,\mu\Phi_0/\sqrt{\mathrm{Hz}} \Rightarrow (23-35)\,\mathrm{pA}/\sqrt{\mathrm{Hz}}$

HOLMES multiplexing readout: current status

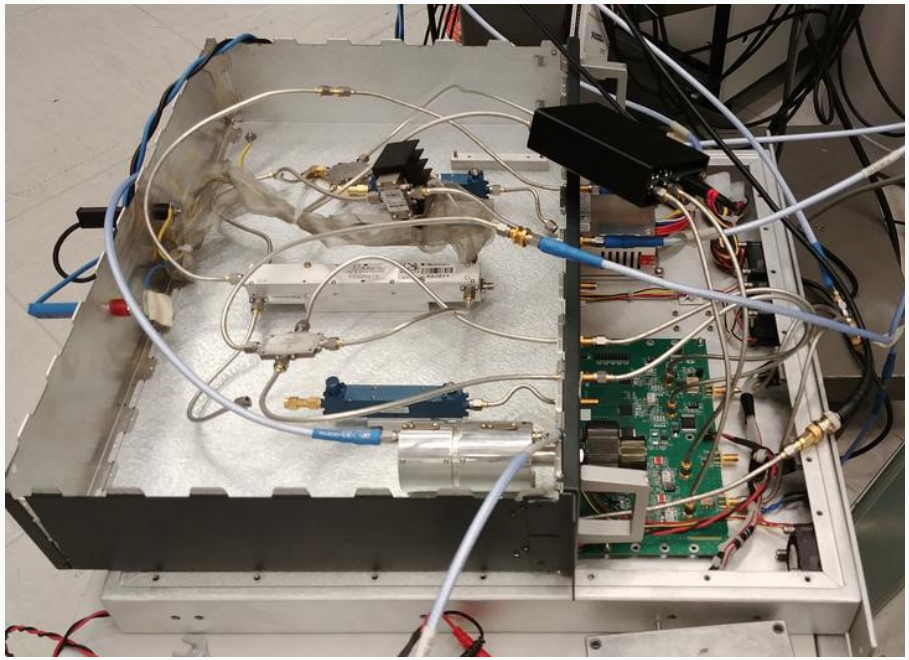

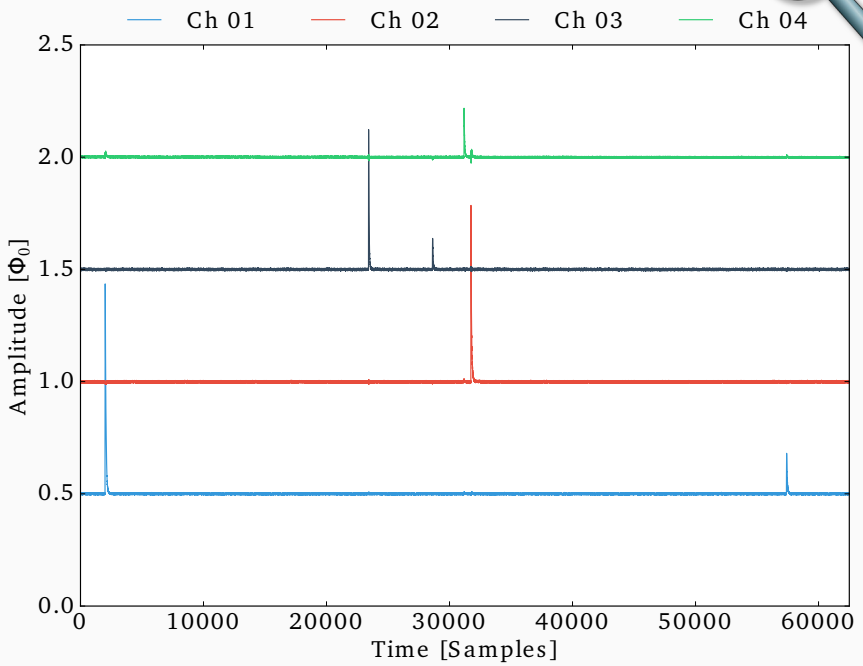

- $1 \times$ ROACH2+MUSIC ADC/DAC boards;
- $1 \times$ custom intermediate frequency (IF) circuitry for up/down conversion;
- Working with: $n_{\Phi_0} = 2$, $f_r = 500$ kHz, $f_{\mathrm{ADC}} = 512$, MHz
- 16-channel firmware from NIST (uses only half of available ADC bandwidth);
- 4 pixels measurements $\Rightarrow$ limited by available tone power;

  needed power: -75/-70 dBm/tones at the multiplexer input

  : -35/-30 dBm/tones at the IF circuitry RF output;

HOLMES: detectors characterization results

Fluorescence source used to test the detectors response

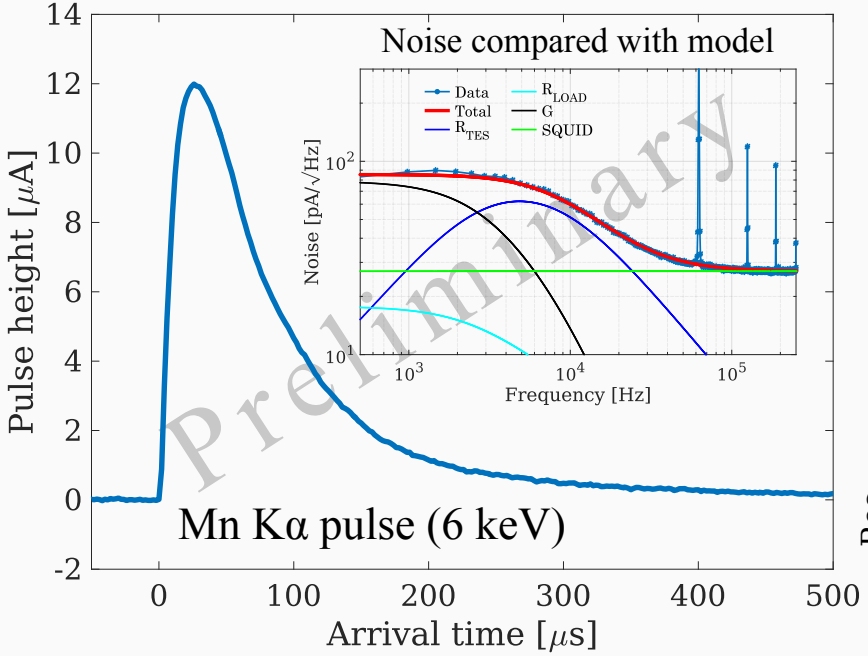

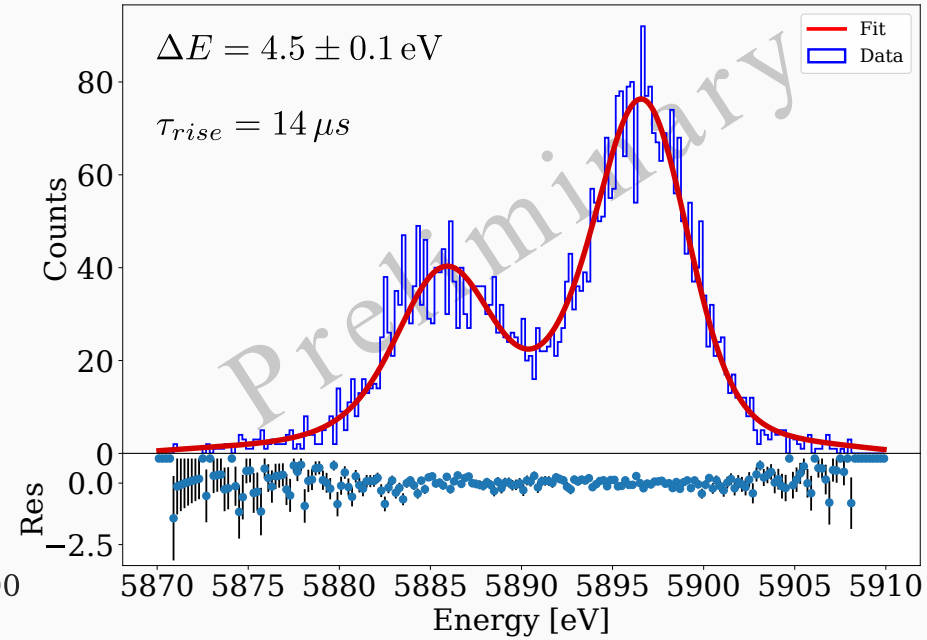

4 detector satisfied the HOLMES requirements

TES #	ΔE_{Al} [eV] (1486 eV)	ΔE_{Cl} [eV] (2622 eV)	ΔE_{Ca} [eV] (3691 eV)	ΔE_{Mn} [eV] (5899 eV)	τ_{rise} [μs]	τ_{short} [μs]	τ_{long} [μs]
2	8.6 ± 0.3	8.8 ± 0.7	7.8 ± 0.2	8.3 ± 0.3	11	56	220
6	6 ± 1	6.0 ± 0.4	6.4 ± 0.4	6.2 ± 0.4	12	34	170
8	4.5 ± 0.3	5.0 ± 0.5	5.0 ± 0.2	4.5 ± 0.1	13	54	220
11	4.3 ± 0.3	4.5 ± 0.3	4.6 ± 0.3		14	32	180

HOLMES: next steps

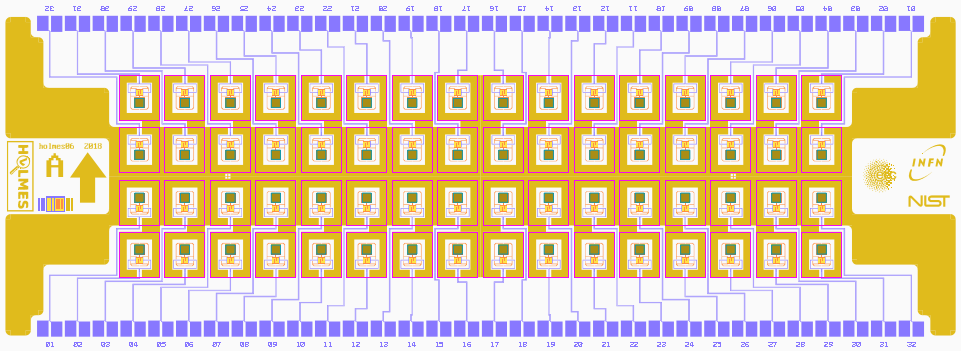

- ^{2nd}detectors generation in production at NIST (slight delay due to government shutdown in US)
  - 4×16 linear sub-array designed for high implant efficiency;
  - First production with sensor/absorber with few differences for determining the better pixel baseline;
  - Second production with pixel baseline implemented and with ^{163}Ho-implanted absorber;
- 4 multiplexer chips with different bandwidht produced at NIST and ready to be send in Milano;
- 64-channel read out and multiplexing system development started in 2018;
  - Based on the 2 ROACH2 systems ($f_{ADC} = 512\,MHz$)
  - Semicommercial up/down converter system able to drive 32 microresonator/board
- ^{163}Ho implanted activity optimized during 2019
  - first high ^{163}Ho activity array running in 2019
  - 1 month of 2 (4×16)-sub array data taking can provide a statistical sensitivity $m_\nu \leq 10$ eV

Conclusion

HOLMES

- The measurement of the end point of nuclear beta or electron capture (EC) decays spectra is the only model-independent;
- The goal of the next future experiments is the sub-eV neutrino mass sensitivity;
- TES x-ray microcalorimeters have already demonstrated high resolution and fast response $\Rightarrow$ large array of these detectors are suitable for the direct measurement of neutrino mass;
- The HOLMES experiment will performe a direct measurment of the nuetrino mass by using microcalorimenter with absorber ^{163}Ho-implanted
  - 100 MBq of ^{163}Ho produced $\Rightarrow$ enough for R&D and 512 pixels;
  - First ^{163}Ho implanting in array absorber running in 2019;
  - 64-channel read out and multiplexing system ready in 2019;
- First physics measurement from the first two sub-array foreseen from 2019;
- Final 1024-pixel configuration will follow;

Backup Slides

Neutrino: known facts

HOLMES

- The discovery of neutrino flavor oscillations has provided convincing evidence for non-zero neutrino masses and leptonic mixing
  - 3 active neutrino flavors: ν_e, ν_μ, ν_τ;
  - Neutrino flavor states are mixture of mass states: ν_1, ν_2, ν_3

$$|\nu_\alpha\rangle = \sum_j U_{\alpha j} |\nu_j\rangle \text{ with } \begin{cases} |\nu_\alpha\rangle & \text{: Flavor weak eigenstate;} \\ U_{\alpha j} & \text{: Neutrino mixing matrix;} \\ |\nu_j\rangle & \text{: Mass eigenstate.} \end{cases}$$

- In a three neutrino model, these oscillations are described by:
  - three angles: $\theta_{12}, \theta_{23}, \theta_{13}$;
  - two mass splittings: $\Delta m^2_{12}, |\Delta m^2_{23}|$;
    Δm^2_{12}: solar+reactor
    $|\Delta m^2_{23}|$: atmospheric+accelerator
  - one CP violating phase: δ_{CP};
  - two Majorana phases: α_1, α_1.
    physically meaningful only if neutrinos are Majorana particles

- Global analysis with different sources and different experimental techiniques:

$$U = \underbrace{\begin{bmatrix} 1 & 0 & 0 \\ 0 & c_{23} & s_{23} \\ 0 & -s_{23} & c_{23} \end{bmatrix}}_{\text{Atmospheric and accelerator experiments}} \cdot \underbrace{\begin{bmatrix} c_{13} & 0 & s_{13}e^{-i\delta_{CP}} \\ 0 & 1 & 0 \\ -s_{13}e^{-i\delta_{CP}} & 0 & c_{13} \end{bmatrix}}_{\text{Reactor and accelerator experiments}} \cdot \underbrace{\begin{bmatrix} c_{12} & s_{12} & 0 \\ -s_{12} & c_{12} & 0 \\ 0 & 0 & 1 \end{bmatrix}}_{\text{Solar and accelator experiments}} \cdot \underbrace{\begin{bmatrix} e^{-i\alpha_1} & 0 & 0 \\ 0 & e^{-i\alpha_2} & 0 \\ 0 & 0 & 1 \end{bmatrix}}_{0\nu\beta\beta \text{ experiments}}$$

$$\Delta m^2_{ij} = m^2_i - m^2_j \ , \ s_{ij} = \sin\theta_{ij} \ , \ c_{ij} = \cos\theta_{ij}$$

Neutrino: global analysis

HOLMES

parameter	Best-fit ± 1σ	2σ range	3σ range
Δm^2_{21} [10^{-5}eV^2]	$7.55^{+0.20}_{-0.16}$	7.20–7.94	7.05–8.14
$\lvert\Delta m^2_{31}\rvert$ [10^{-3}eV^2] (NO)	2.50 ± 0.03	2.44–2.57	2.41–2.60
$\lvert\Delta m^2_{31}\rvert$ [10^{-3}eV^2] (IO)	$2.42^{+0.03}_{-0.04}$	2.34–2.47	2.31–2.51
$\sin^2\theta_{12}/10^{-1}$	$3.20^{+0.20}_{-0.16}$	2.89–3.59	2.73–3.79
$\sin^2\theta_{23}/10^{-1}$ (NO)	$5.47^{+0.20}_{-0.30}$	4.67–5.83	4.45–5.99
$\sin^2\theta_{23}/10^{-1}$ (IO)	$5.51^{+0.18}_{-0.30}$	4.91–5.84	4.53–5.98
$\sin^2\theta_{13}/10^{-2}$ (NO)	$2.160^{+0.083}_{-0.069}$	2.03–2.34	1.96–2.41
$\sin^2\theta_{13}/10^{-2}$ (IO)	$2.220^{+0.074}_{-0.076}$	2.07–2.36	1.99–2.44
δ_{CP}/π (NO)	$1.32^{+0.21}_{-0.15}$	1.01–1.75	0.87–1.94
δ_{CP}/π (IO)	$1.56^{+0.13}_{-0.15}$	1.27–1.82	1.12–1.94

The results for inverted mass ordering were calculated with respect to this mass ordering.

- $\Delta m^2_{21} = \Delta m^2_{\odot} \simeq 75\,\mu\,\mathrm{eV}^2$
- $|\Delta m^2_{31}| = |\Delta m^2_{\mathrm{atm}}| \simeq (2.4 - 2.5)\,\mathrm{m\,eV}^2$
- $\theta_{12} = \theta_{\odot} \simeq 35^\circ$
- $\theta_{13} = \simeq 8.5^\circ$
- $\theta_{23} = \Delta m^2_{\mathrm{atm}} \simeq 45^\circ$

- The sign of Δm^2_{31} is currently unknown;
- The octant of θ_{23} is currently unknown (low-octant: $\theta_{23} < 45^\circ$, high-octant: $\theta_{23} > 45^\circ$)
- δ_{CP} known in the range $[\pi, 2\pi]$;
- α_1 and α_2 are currently unknown;

(more details on Front. Astron. Space Sci. 5 (2018) 36 and Phys. Lett. B 782 (2018) 633–640)

Neutrino: unknown facts

HOLMES

Despite the good precision that neutrino experiments have reached in the recent years, many neutrino properties remain still unknown.

- the absolute scale of neutrino masses
  - $m_e < 2.05$ eV (Phys.Rev. D84 (2011) 112003)
  - $m_\mu < 0.17$ MeV (Phys. Rev. D53 (1996) 6065-6077)
  - $m_\tau < 18.2$ MeV (Eur. Phys. J. C2 (1998) 395–406)

- the type of the neutrino mass spectrum on the absolute scale of neutrino masses
  - Normal hierarchical (NH): $m_1 \ll (<) m_2 \ll m_3 \Rightarrow \Delta m^2_{32,31} > 0$
  - Inverted hierarchical (IH): $m_3 \ll m_1 \lesssim m_2 \Rightarrow \Delta m^2_{32,31} < 0$

- the neutrino nature:
  - Dirac particle: $\nu \neq \overline{\nu}$
  - Majorana particle: $\nu = \overline{\nu}$

- the existence of CP violation in the leptonic sector;
  - if $\delta_{CP} \neq 0 \Rightarrow$ neutrino vs. antineutrino appearance (but not disappearance) should have different rates

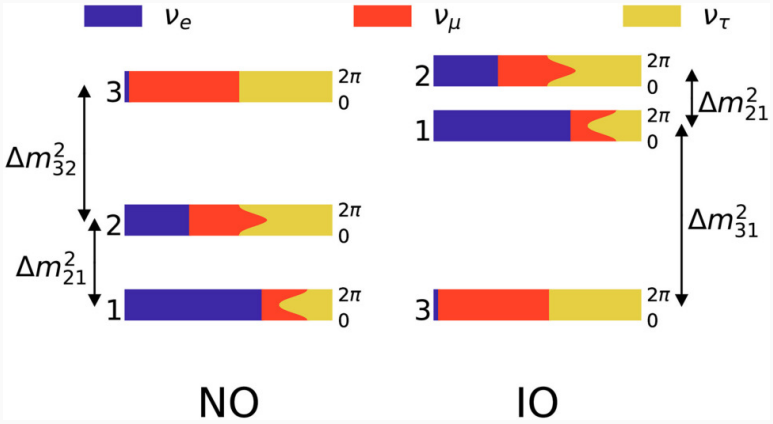

Microwave rf-SQUID multiplexing: flux-ramp modulation

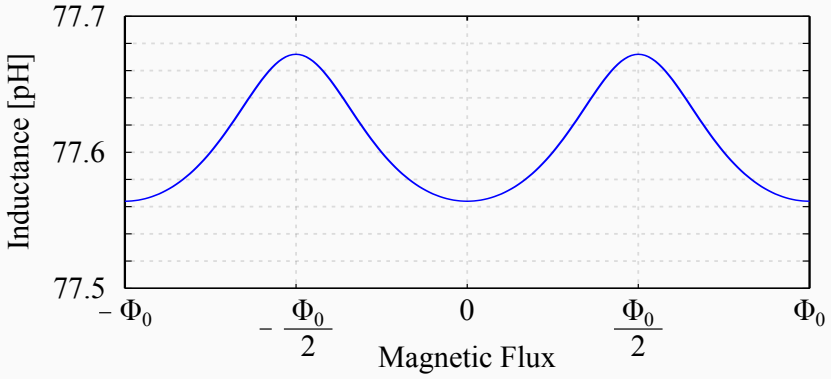

$$\Phi = \Phi_{\mathrm{TES}} + \Phi_{\mathrm{ramp}}$$

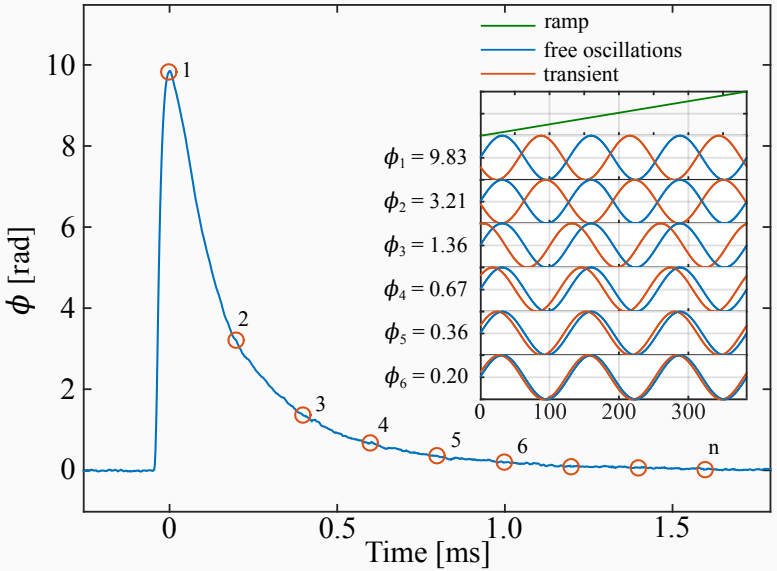

- A flux-ramp modulation is applied by a common line inductively coupled to all SQUIDs
- The signal is reconstructed by comparing the phase shift caused by the interaction of the radiation in the TES, with the free oscillation of the SQUID, when the TES is not biased;
- Each ramp acquisition represents a sample in the reconscruted phase signal: $f_{\mathrm{sample}} = f_{\mathrm{ramp}}$
- Necessary resonator bandwidth per flux ramp: $\Delta f_{\mathrm{BW}} \geq 2\, n_{\Phi_0}\, f_{\mathrm{ramp}}$
- To avoid cross talk $\Rightarrow$ spacing between resonances $S > \Delta f_{\mathrm{BW}}$
- To avoid distortions $\Rightarrow f_{\mathrm{ramp}} > 10/\tau_{\mathrm{rise}}$ (potentially reduced by a factor 2);
- Minimum number of flux cycles per ramp: $n_{\Phi_0} = 2$ (possibly 1.1 with different ramp shape).

HOLMES multiplexing readout: 64 channel readout

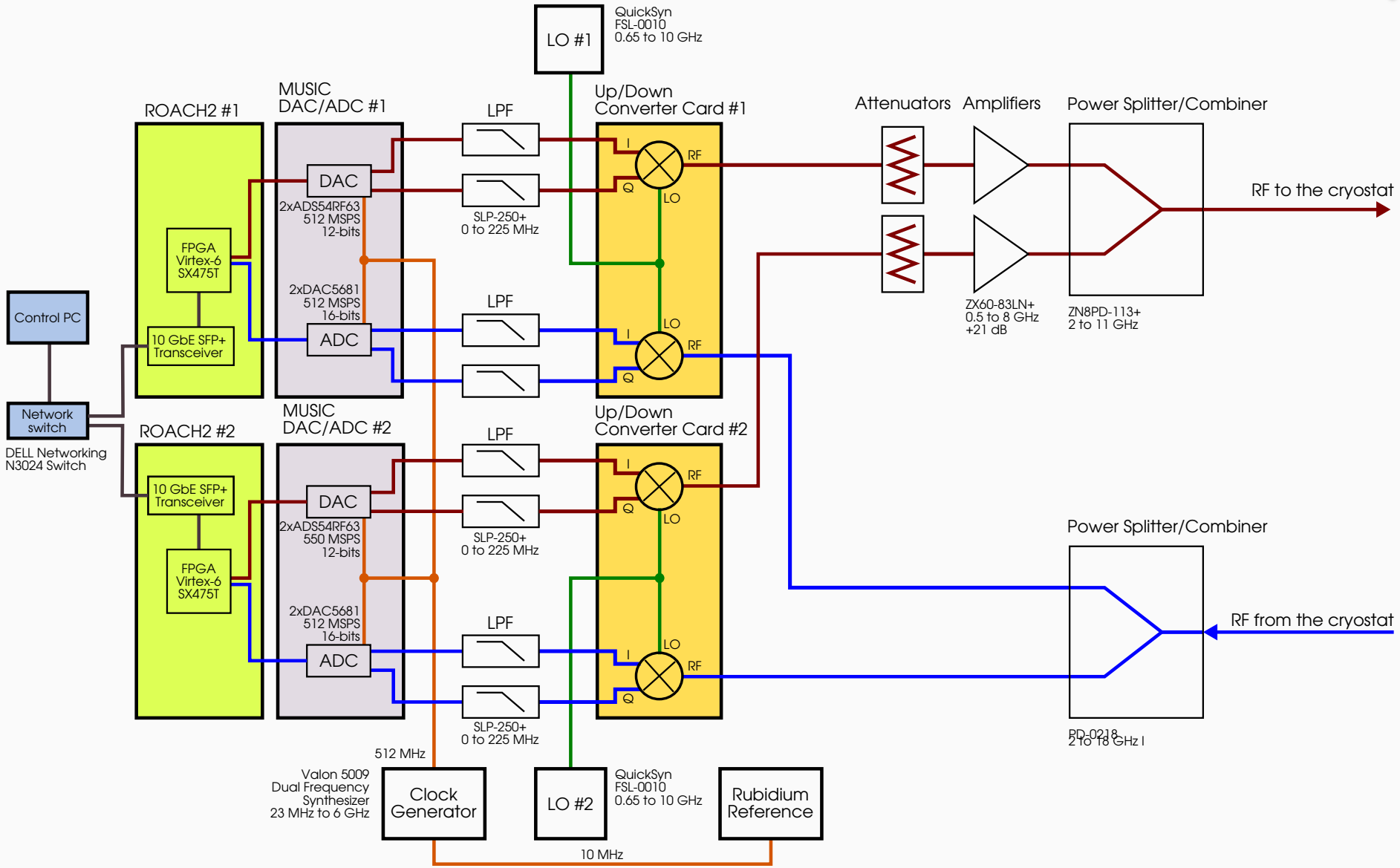

PXI Block Up/Down Converter by Polyphase Microwave

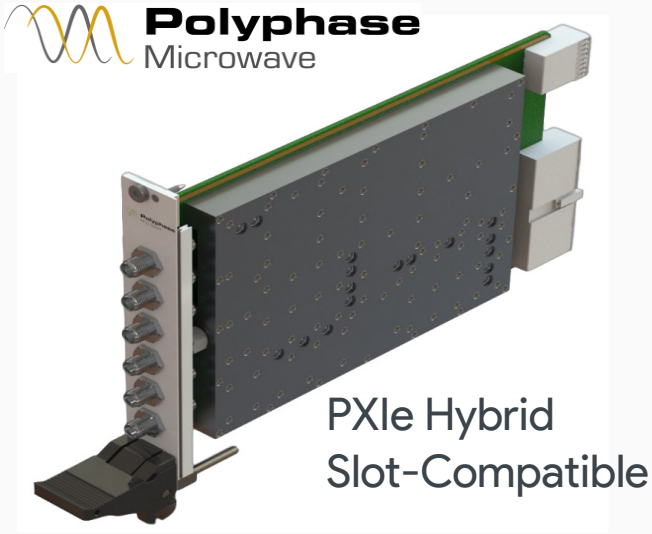

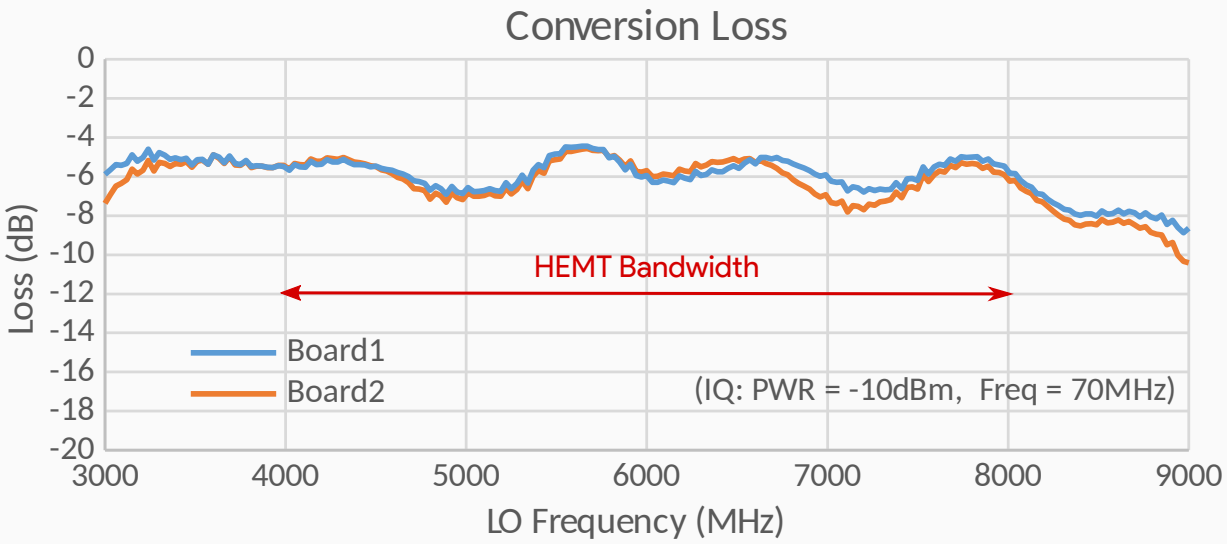

- Commercial design but customized to match the HOLMES requirements;
- Working in C-Band (4.0 to 8.0) GHz $\Rightarrow$ fully compatible with the HEMT bandwidth;
- Internal or External LO Synthesizers;
- 30 dB/ 1dB step programmable RF Attenuation;
- Total loss around -7 dB $\Rightarrow$ compatible with the power needed to drive 32 microresonators.

First two boards in Milano

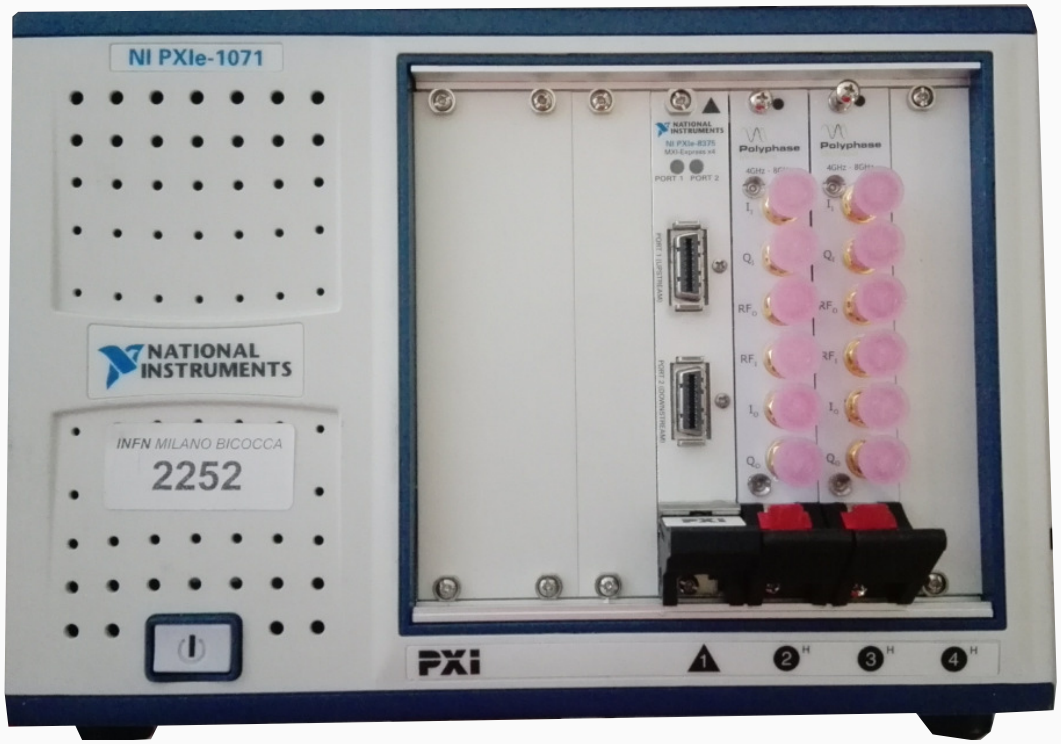

- Commercial design but customized to match the HOLMES requirements;
- First two boards delivered in Milano on August 1.
- First integration in the HOLMES readout on September 26
- First tests performed without cryogenic multiplexer;
- Tones characterization with power spectrum analyzer in progress;

Increasing the multiplexing factor

HOLMES

- The multiplexing factor is limited by the read out bandwidth f_{ADC};
- The current read-out and multiplexing system is based on the ROACH2 system:
  - developed inside the MKIDs community and then also used for TESs;
  - very robust system but with limitated bandwidth: 2 ADCs with $f_{ADC} = 512$ MHz, 12-bit;
  - despite it was developed for the MUSIC experiment in 2010 it is currently the only one ready-to-use system;
- Other system are currently in develpoment:
  - fMESSI @Fermilab (USBC/Fermilab collaboration): 2 ADCs with $f_{ADC} = 2$ GHz, 16-bit;
  - SMuRF @SLAC: 4 ADCs with $f_{ADC} = 2.5$ GHz, 14-bit;
- Starting from 2018 also a commercial solution is available:
  - Zynq UltraScale+ RFSoC (chip developed by Xilinx);
  - 8 ADCs with $f_{ADC} = 4$ GHz, 12-bit
  - Ideally one chip can replace a large number of ROACH2 boards;
  - A board development is not needed since the demo kit (Zynq UltraScale+ RFSoC ZCU111) is read to use. Cost $8'995 (from Xilinx website);
  - All the groups involved in the development of microwave readout (NIST/UCSB/Fermilab/...) have been have been purchased the demo kit;